Computational Design of Creep-Resistant Alloys and Experimental Validation in Ferritic Superalloys

Investigators: Peter K. Liaw[1], Mark D. Asta[2], Gautam Ghosh[3], David C. Dunand[3], Morris E. Fine[3], and Chain T. Liu[4]

Ph.D. Students: Hong Ding[2], Shenyan Huang[1], Michael Rawings[3], Zhiqian Sun[1], and Zhenke Teng[1]

Research Associate: Gongyao Wang[1]

1. Department of Materials Science and Engineering, The University of Tennessee (UT), Knoxville, TN 37996, USA
2. Department of Materials Science and Engineering, University of California (UC), Berkeley, CA 94720, USA
3. Department of Materials Science and Engineering, Northwestern University (NU), Evanston, IL 60208-3108, USA
4. Department of Materials Engineering, Auburn University, Auburn, AL 36849, USA

Acknowledgements

We are very grateful to:

(1) Richard Dunst,

(2) Veto Cedro, and

(3) Patricia Rawls for their kind support.

(4) National Energy Technology Laboratory (NETL) for sponsoring this project.

Outline

- Technical Background of the Project
- Statement of Project Objectives
- Previous Results
- Technical Approach to Achieve the Project Goals
- Conclusions

Technical Background of the Project

Ferritic Alloys as Candidates for Steam Turbine (1)

Why ferritic steels? Why not Ni-based alloys?

- 80% of all electricity generation in the world is by use of steam turbines. Low cost materials are required.

- The materials with good thermal conductivity and low thermal expansion are preferable for thick section components of the steam turbine.

	Thermal Expansion Coefficient [2]	Thermal Conductivity[3]	Cost ($/t) [4]
Ferritic steel	1.0×10^{-5} K^{-1}	50 W/(m·K)	< $900
Ni-based superalloy	1.8×10^{-5} K^{-1}	21 W/(m·K)	> $40K

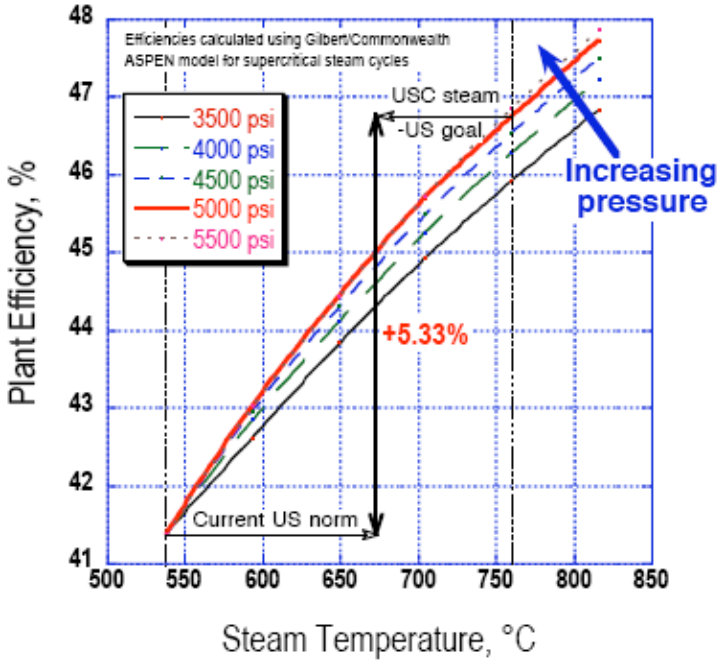

P. Maziasz, I. Wright, J. Shingledecker, T. Gibbons, R. Romanosky, *Proceedings from the fourth international conference on advances for materials technology for fossil power plants* 2005.

[1] http://en.wikipedia.org/wiki/Steam_turbine
[2] http://www.handyharmancanada.com/TheBrazingBook/comparis.htm
[3] http://en.wikipedia.org/wiki/List_of_thermal_conductivities
[4] http://www.ttiinc.com/page/ME_Materials

Ferritic Alloys as Candidates for Steam Turbine (2)

Why B2 or/and $L2_1$ precipitates strengthened ferritic steels?

Phase	Structure	Lattice Parameter (nm)
α-Fe	Body-Centered-Cubic (BCC)	0.28665
NiAl	B2 (ordered BCC)	0.28864
FeAl	B2 (ordered BCC)	0.289
Ni_2TiAl	$L2_1$	0.5865

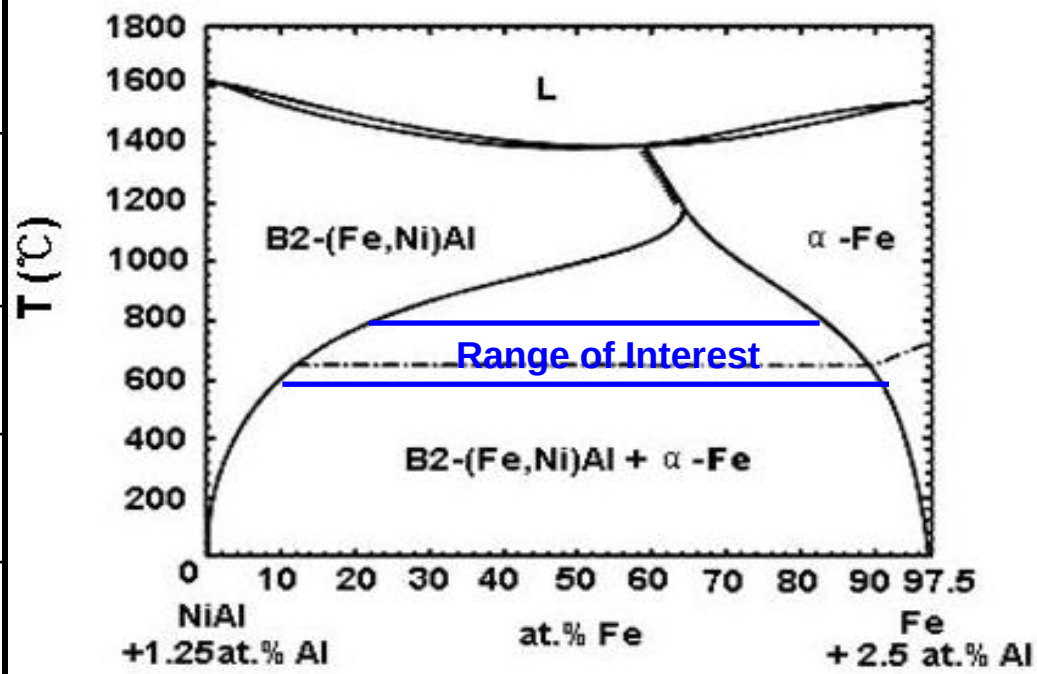

Ordered B2 (Fe, Ni)Al-type and ordered $L2_1$ Ni_2TiAl-type precipitates can form in a coherent-coplanar orientation, providing the possibility of achieving a Fe-based analogue to the Ni-based superalloys.

Ferritic Alloys as Candidates for Steam Turbine (3)

Why B2 or/and $L2_1$ precipitates strengthened ferritic steels?

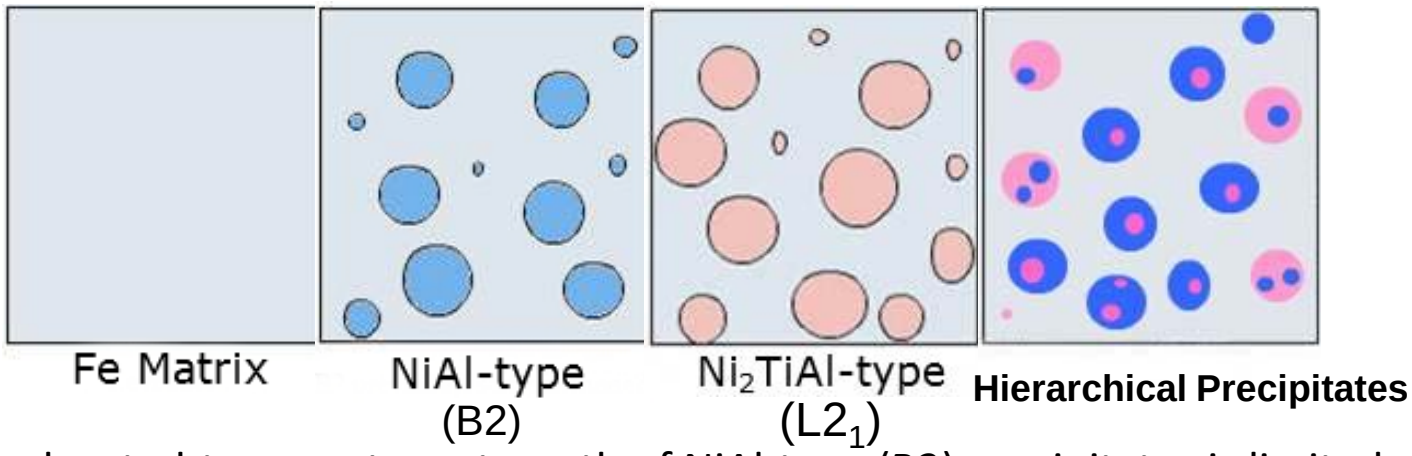

- The elevated-temperature strength of NiAl-type (B2) precipitates is limited by their properties.
- The creep strength (defined as the stress to maintain a steady-state rate of 10^{-7} s^{-1}) of Ni_2TiAl ($L2_1$) between 1, 026 to 1, 273 K is about three times that of NiAl in its most creep-resistant form.
- The creep strength of NiAl-Ni_2TiAl two-phase alloys are more creep resistant than either of the phases in its monolithic form and at least comparable to the Ni-based superalloy, MAR-M200 (nominal composition wt.%: Cr 9.0; Co 10.0; W 12.5; Nb 1.0; Ti 2.0; Al 5.0; C 0.15; B 0.015; Ni balance).

P. R. Strutt, R. S. Polvani, and J. C. Ingram. Metallurgical Transaction A. 7, 23 (1976)
R. S. Polvani, W. S. Tzeng, and P. R. Strutt. Metallurgical Transaction A. 7, 33 (1976)

Project Objectives

- **Objective 1:** to develop and integrate modern computational tools and algorithms required to assist in the optimization of creep properties of high-temperature alloys for fossil-energy applications
  - Integrate tools and methods associated with predictive first-principles calculations, computational thermodynamic and kinetic modeling, and meso-scale dislocation-dynamics simulations.
- **Objective 2:** to achieve a fundamental understanding of the processing-microstructure-property-performance links underlying the creep behavior of novel ferritic superalloys strengthened by *B2 and/or* $L2_1$ intermetallics.
  - validate some of the computational results by measuring selected microstructural attributes in representative model ferritic superalloys with a hierarchical microstructure

Previous Results

Conceptual Microstructures (1)

- Dispersion of NiAl-type precipitates in an Fe matrix

TEM BF showing coherency strain contrast

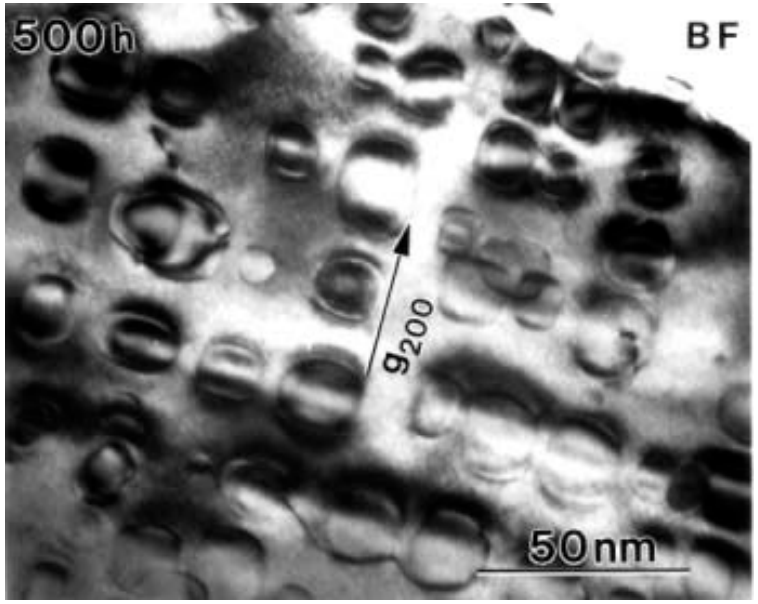

TEM DF (using 100-type reflections) showing B2 precipitates

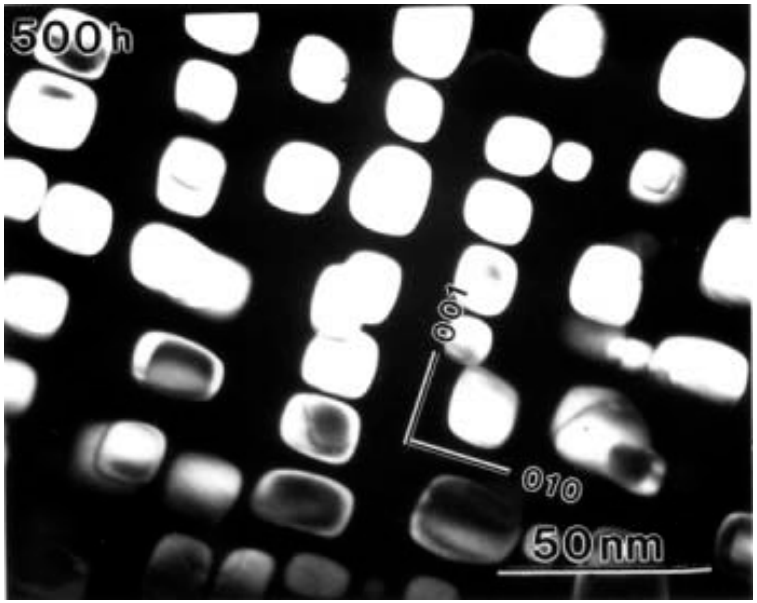

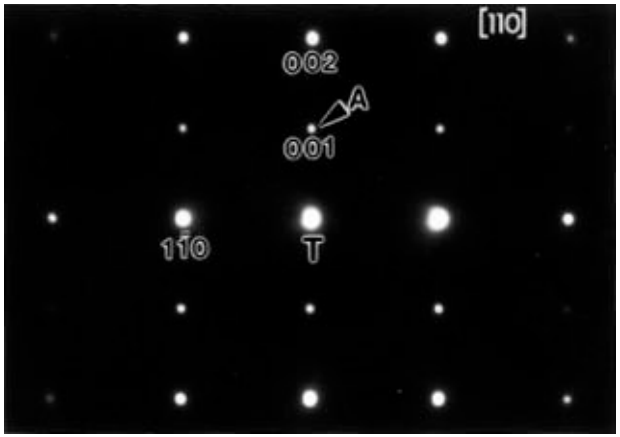

Alloy composition: Fe-8.08Al-12.2 Cr-1.9Mo-18.2Ni (wt. %)

G. Ghosh, Unpublished research, NU

Conceptual Microstructures (2)

- A hierarchical microstructure: NiAl-type and Ni_2TiAl-type precipitates

TEM BF micrograph

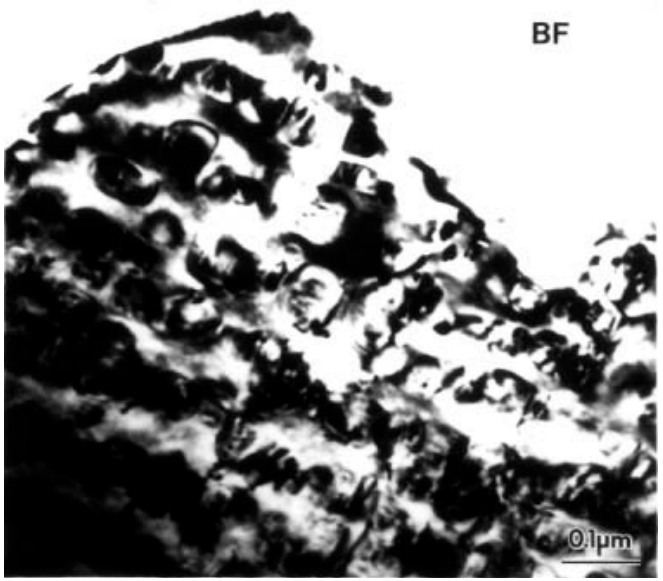

TEM DP showing reflections of both *B*2 and $L2_1$ type structures

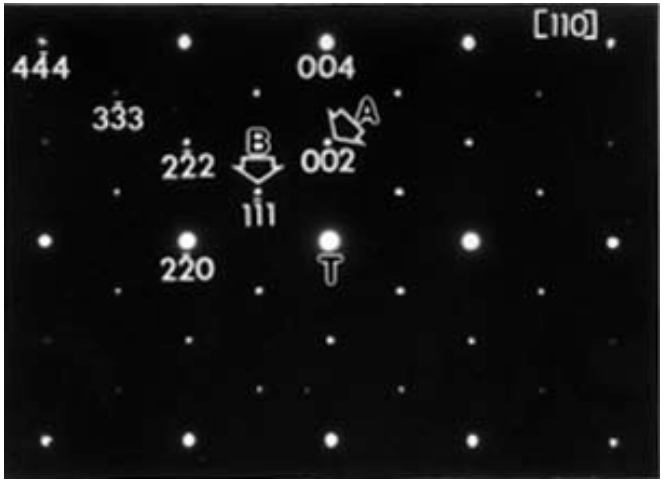

Alloy composition: Fe-8.08Al-12.2Cr-1.9Mo-18.2Ni-2Ti (wt. %)

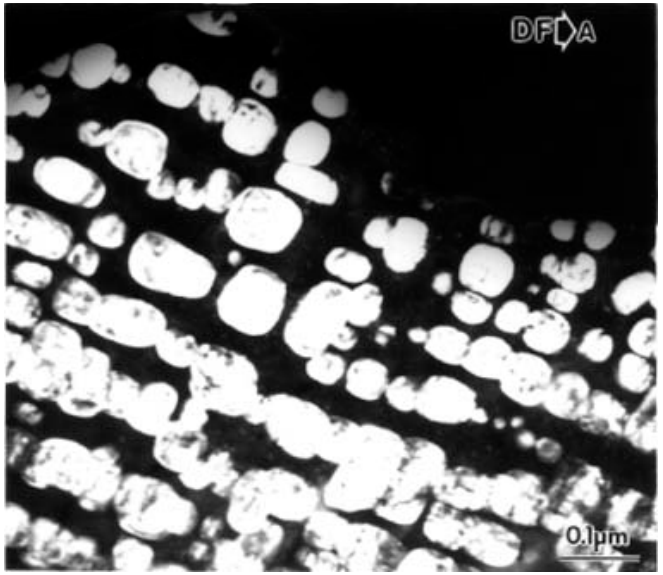

TEM DF using (200)-type $B2/L2_1$ spots

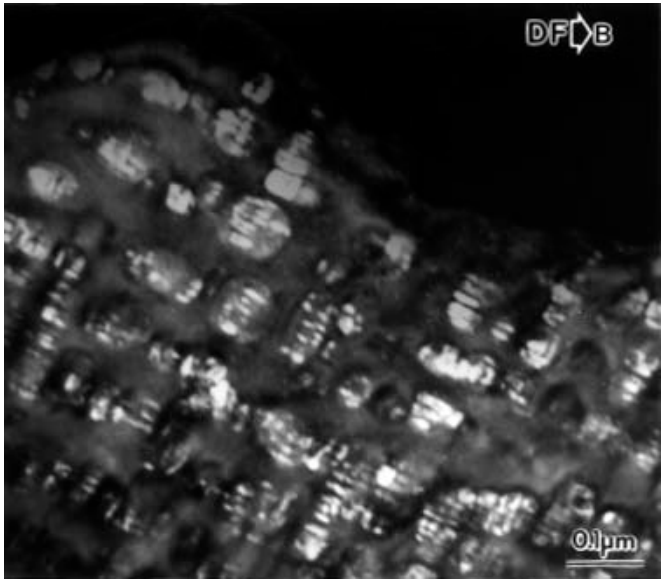

TEM DF using (111)-type $L2_1$ spots (unique)

G. Ghosh, Unpublished research, NU

Atom Probe Tomography (APT) Characterizations

Ferritic steel reinforced by NiAl-type precipitates

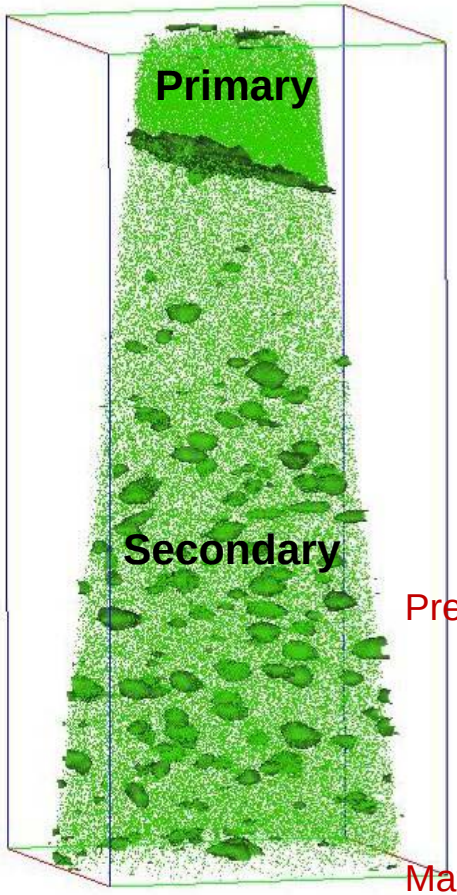

15 at.% Al iso-concentration surface

10 nm

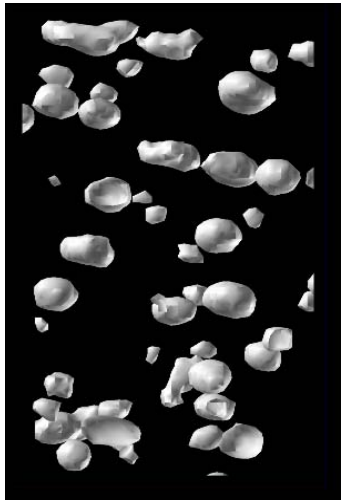

Morphology of secondary precipitates

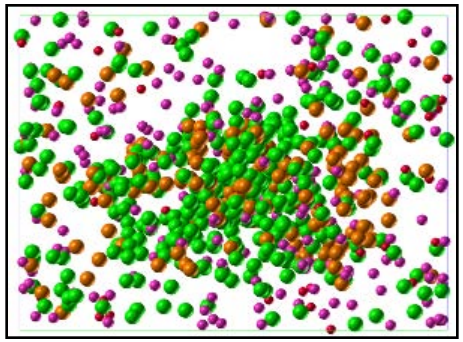

Atom map of a selected secondary precipitate

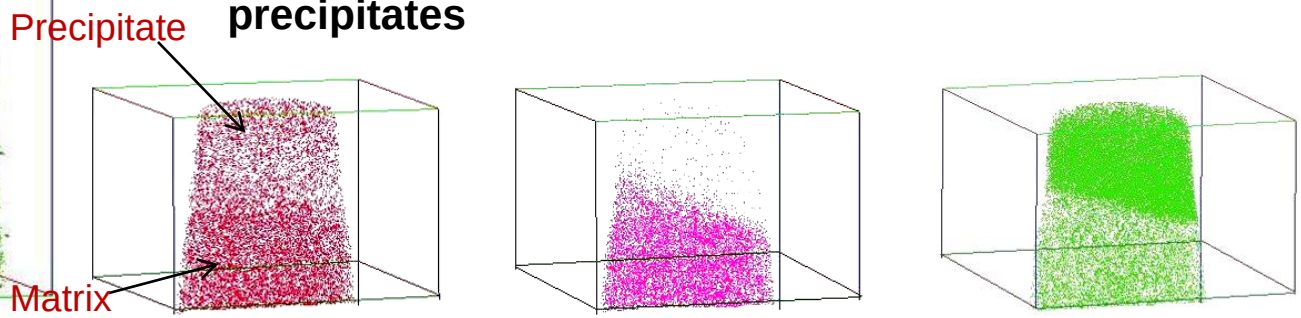

Mo atom map | Cr atom map | Al atom map

APT revealed a duplex precipitation of NiAl particles: primary with an diameter of 130 nm ($Ni_{41.2}Al_{43.6}Fe_{12.7}Cr_{0.8}Mo_{1.4}$) and secondary with an diameter of 3 nm ($Ni_{26.3}Al_{41.6}Fe_{26.9}Cr_{3.3}Mo_{1.7}$). The overall composition is Fe-12.7 Al-9 Ni-10.2 Cr-1.9 Mo, at.%.

Z.K. Teng, M.K. Miller, G. Ghosh, C.T. Liu, S. Huang, K.F. Russell, M.F. Fine, and P.K .Liaw. Scripta Mater. 63, 61 (2010).

Proposed Research and Detailed Technical Approach to Achieve the Project Goals

Integrated Computational Approach

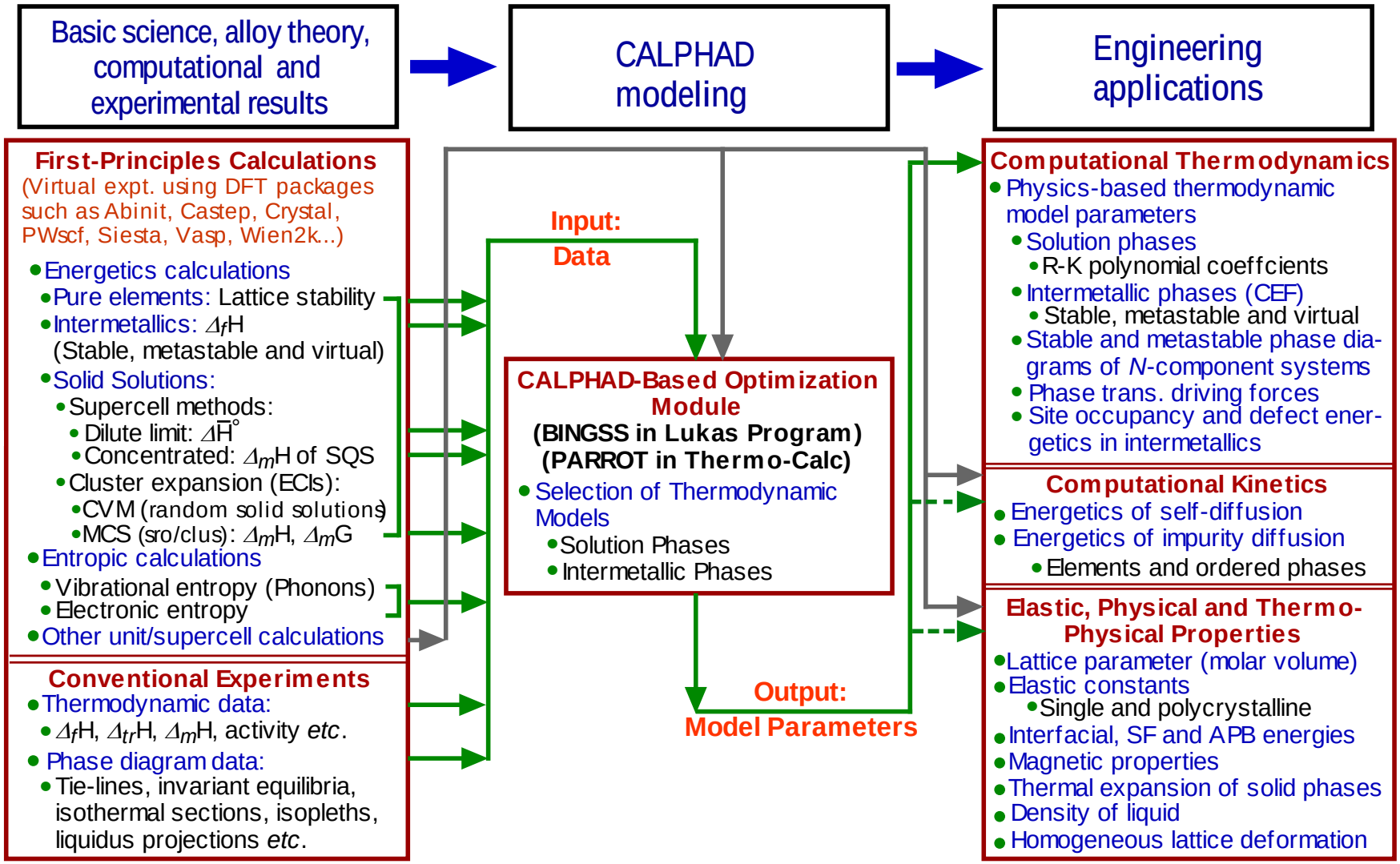

G. Ghosh, A. van de Walle, and M. Asta. Acta Mater., 56, 3202 (2008)

1.1 Proposed Research

- Principal computational tools
  - Vienna Ab-initio Simulation Package (VASP): total energy and electronic structures
  - Alloy Theoretic Automated Toolkit (ATAT): cluster expansion (energy, lattice parameter, elastic properties of disordered solid solutions), Monte Carlo simulation (diffuse interface energy)
  - Thermo-Calc: multi-component, multi-phase equilibria
    - Predictive accuracy depends on the accuracy of database
  - DICTRA: multi-component, multi-phase diffusion
    - Predictive accuracy depends on the accuracy of database

- Hardware resources
  - QUEST cluster (NU)
  - TeraGrid resources
  - NERSC resources (Lawrence Berkeley National Laboratory)

2.1 Proposed Research: Model for Self and Impurity Diffusivities

Harmonic Transition State Theory Assuming Vacancy Mechanism

$$D_A^B = D_{0A}^{\ B} \exp[-Q_A^B / k_B T]$$

Self Diffusion in α-Fe

$$D_{0Fe}^{\ Fe} = a^2 f_{bcc} \exp\left[\frac{\Delta S_v^f}{k_B}\right] x \left[\prod_{i=1}^{3N-3} \nu_i^{vac} \Big/ \prod_{i=1}^{3N-4} \nu_i^{sad}\right] \qquad Q_{Fe}^{Fe} = \Delta H_v^f + \Delta H_v^{mig,Fe}$$

Impurity Diffusion

$$D_{0Fe}^{\ I} = a^2 f_{Fe}^I \exp\left[\frac{\Delta S_v^f + \Delta S_v^{bind}}{k_B}\right] x \left[\prod_{i=1}^{3N-3} \nu_i^{vac} \Big/ \prod_{i=1}^{3N-4} \nu_i^{sad}\right] \qquad Q_{Fe}^I = \Delta H_v^f + \Delta H_v^{bind} + \Delta H_v^{mig,I}$$

Diffusivity Calculations Require Determinations of:

- Vacancy Formation, Binding and Migration Energies
- Vacancy Formation, Binding and Migration Entropies
- Correlation Factors for Impurity Diffusion

2.2 Proposed Research: Activation Energies

Magnetic Contributions

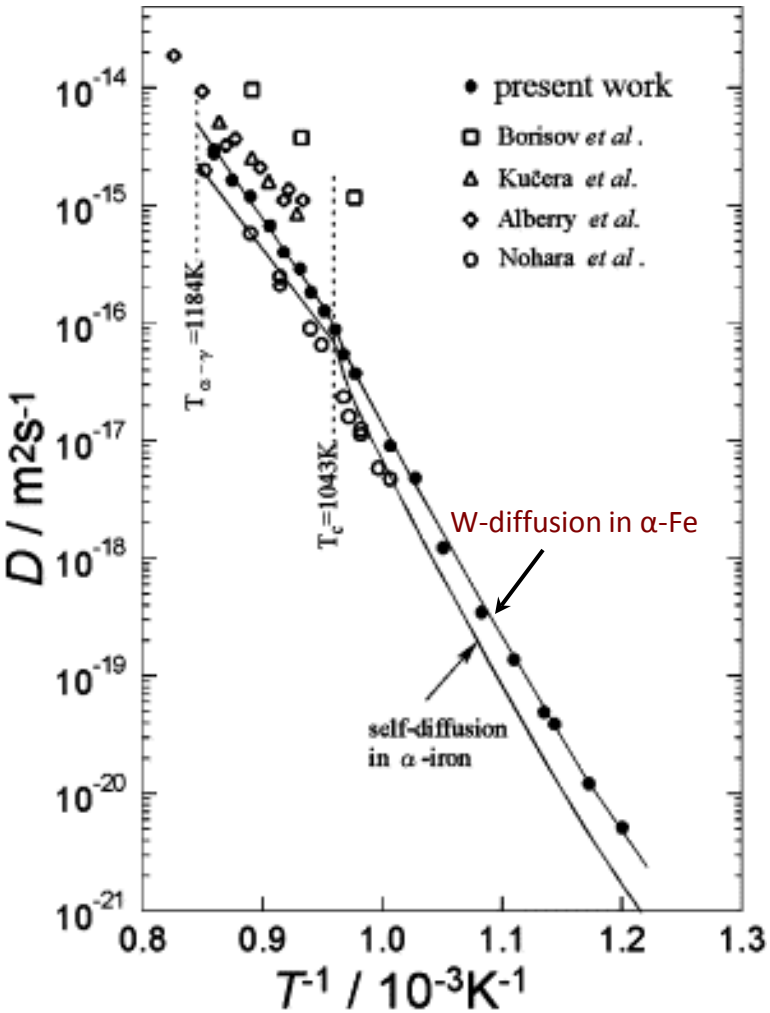

S. Takemoto, H. Nitta, Y. Iijima, and Y. Yamazaki. *Phil Mag.*, 87, 1619 (2007).

Magnetic Contribution in Ferromagnetic Phase

$$Q^F(T) = Q^P\left(1 + s(T)^2\alpha\right)$$

$$s(T) = M(T)/M(0)$$

- α quantifies the influence of magnetic ordering on activation energy, Q
- α measured for relatively few solutes

2.3 Proposed Research: Semi-Empirical Model for α

Empirical Linear Relation: α and Induced Magnetization, ΔM_{12}

$$\Delta M_{12} = \sum_{i=1}^{8} \Delta m_i^{1st\ NN} + \sum_{j=1}^{6} \Delta m_j^{2nd\ NN}$$

S. Takemoto, H. Nitta, Y. Iijima, and Y. Yamazaki. *Phil Mag.*, 87, 1619 (2007).

- Calculate ΔM_{12} for solutes with known α
- Fit linear relationship:

$$\alpha = 0.0586\Delta M_{12} + 0.1591$$

- Predict α for other solutes

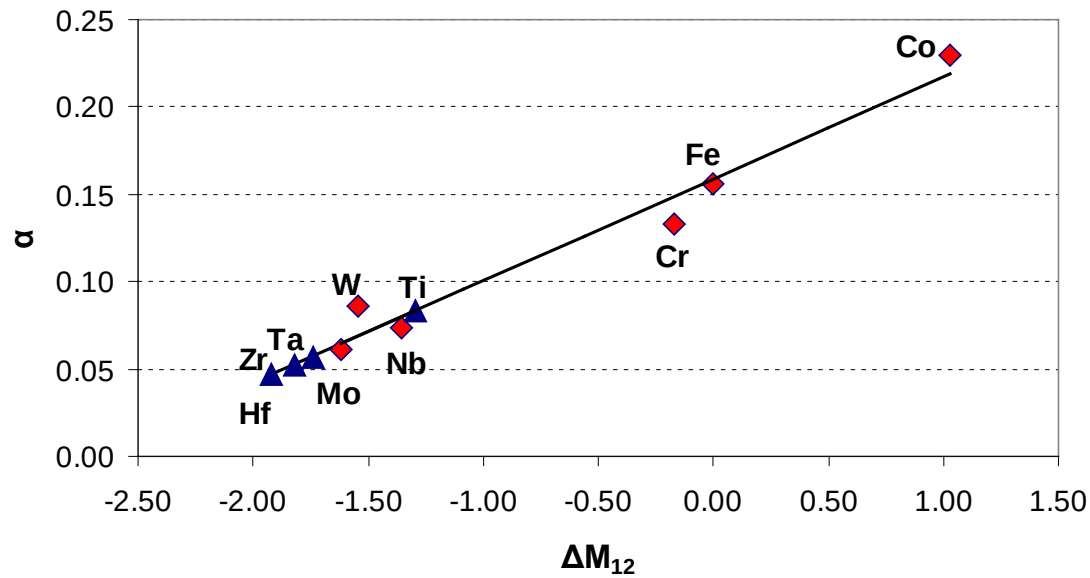

2.4 Proposed Research: Extension of Diffusion Modeling

- Complete systematic calculations of impurity diffusivities for 3d, 4d, and 5d solutes
  - Initial tests underway to increase efficiency of calculations
  - Develop further the model for magnetic effects on activation energies in paramagnetic state using special quasirandom supercell structures to model magnetic disorder

- Extend calculations to concentrated mixtures
  - Compute vacancy-hopping frequencies as a function of chemical environment employing approaches described in previous slides
  - Use results to build up a kinetic-Monte-Carlo simulation for binary systems
  - Compute diffusion coefficients as a function of temperature and concentration from analysis of statistics of random walks for individual atoms (self or tracer diffusion) or for center of mass of atomic positions (interdiffusion)

3.1 Proposed Research: Neutron and Synchrotron Facilities

Spallation Neutron Source, Oak Ridge National Laboratory

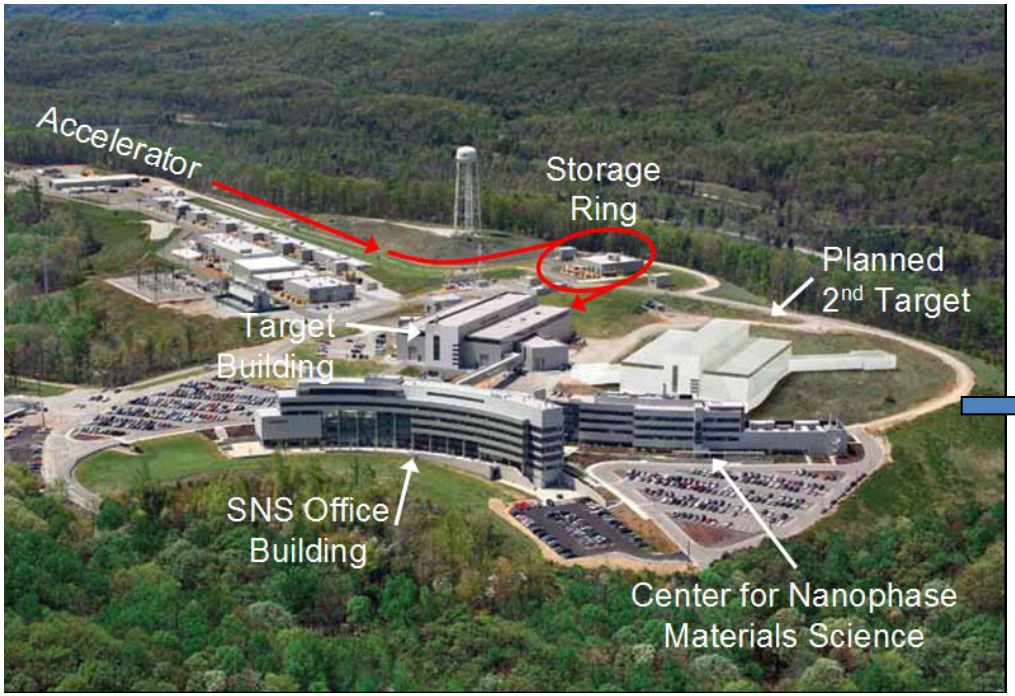

Conceptual design of VULCAN diffractometer

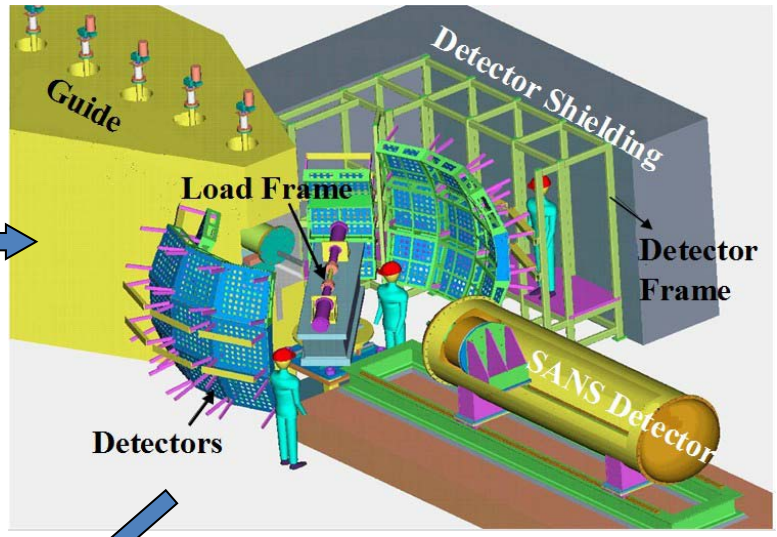

The multifunctional load-frame developed for VULCAN diffractometer

3.2 Proposed Research: Experimental Setup of Ultra-Small-Angle X-Ray Scattering Analysis (USAXS)

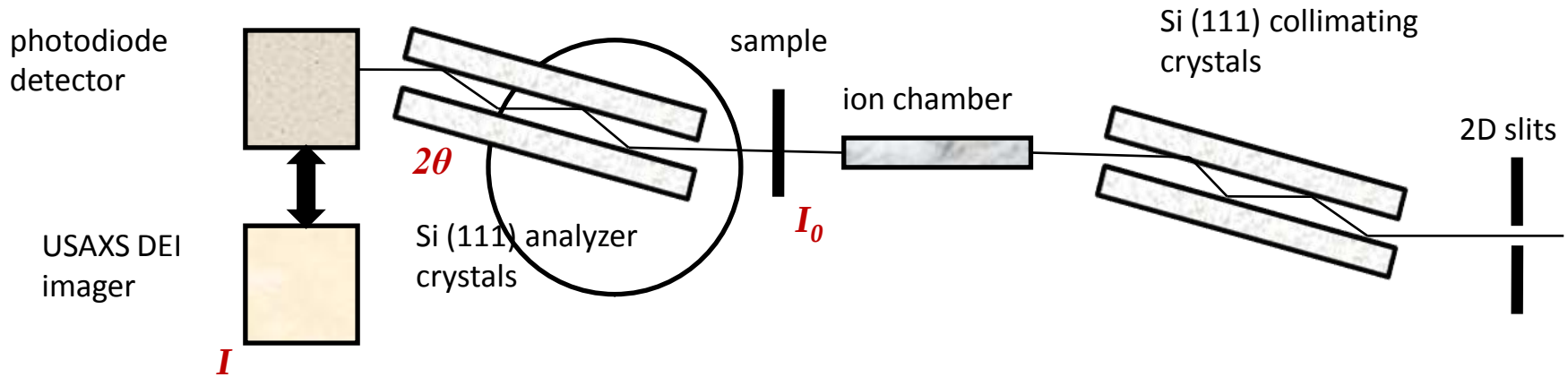

1-D collimated USAXS camera at Advanced Photon Source 15-ID-D, Argonne National Laboratory

Experiment:

- Measured Q range: 10^{-3} ~ 0.5 $Å^{-1}$
- Beam energy: ~ 17 keV
- Beam size: 1.6 x 0.8 mm
- Foil thickness: ~ 50 µm
- Data reduction and desmearing: Irena Package

3.3 Proposed Research: Theoretical Model for USAXS Data Analysis

Absolute intensity -- ***Fourier transformation of electron density***

Non-dilute precipitation: Polydispersity + Interference

Difference in scattering-length density between two phases

Scattering from grain boundaries

Number density of precipitates

Scattering intensity (background)

One population of precipitates

$$I(Q) = n_p |\Delta\rho|^2 P(Q) S(Q) + AQ^{-b} + I_{INC}$$

Form factor – particle size and shape

$$P(Q) = \left(\frac{4\pi}{3}\right)^2 \int F^2(Q,x) \times N(x,R,\delta) \times x^6 dx$$

$$F(Q,x) = [\sin(Qx) - Qx\cos(Qx)]/(Qx)^3$$

$$N(x,R,\delta) = \exp\left[-(x-R)^2/2\delta^2\right]/\sqrt{2\pi\delta^2}$$

Structure factor – inter-particle correlation

$$S(Q,L,\sigma) = 2\left\{\frac{1-\exp\left(-\frac{Q^2\sigma^2}{4}\right)\cos(QL)}{1-2\exp\left(-\frac{Q^2\sigma^2}{4}\right)\cos(QL)+\exp\left(-\frac{Q^2\sigma^2}{2}\right)}\right\}-1$$

Non-linear least-square fitting for 8 parameters: $n_p|\Delta\rho|^2$, I_{INC}, A, R, δ, L, σ, b

3.4 Proposed Research: Quantitative Ultra-Small-Angle X-Ray Scattering Analysis

Ferritic steel reinforced by NiAl-type precipitates

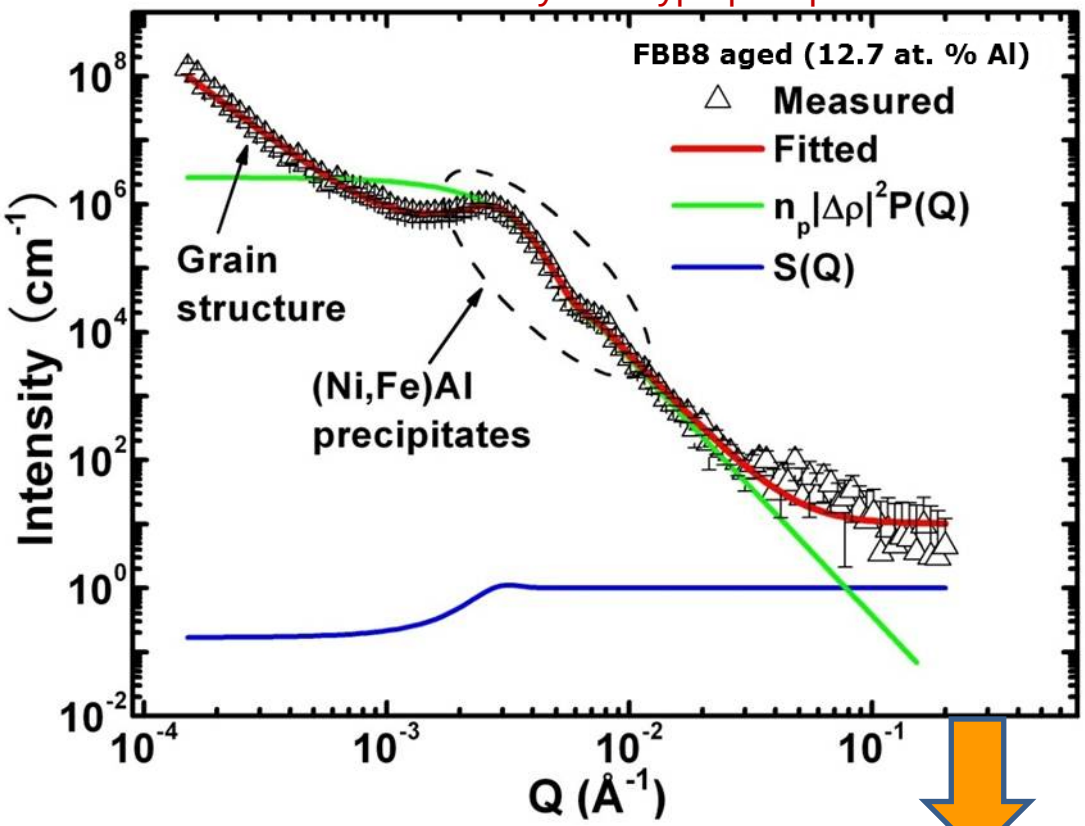

Dark Field Image by 100_{B2} reflection

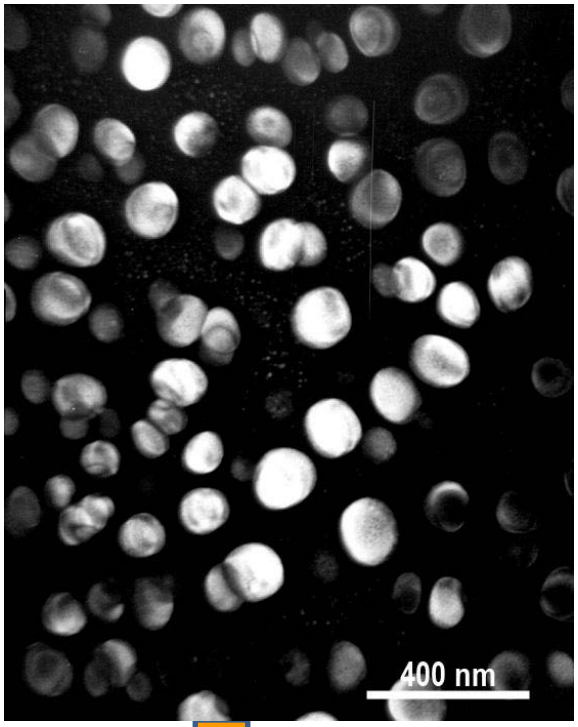

Parameters	USAXS	TEM
Diameter of precipitates	129.8 nm	130 nm
Standard deviation of diameter	30.0 nm	25 nm
Inter-particle spacing	175.0 nm	211 nm
Standard deviation of spacing	101.7 nm	37.5 nm

FBB8: Fe-12.7Al-9Ni-10.2Cr-1.9Mo, at.%.

3.5 Proposed Research: Neutron-Diffraction Studies

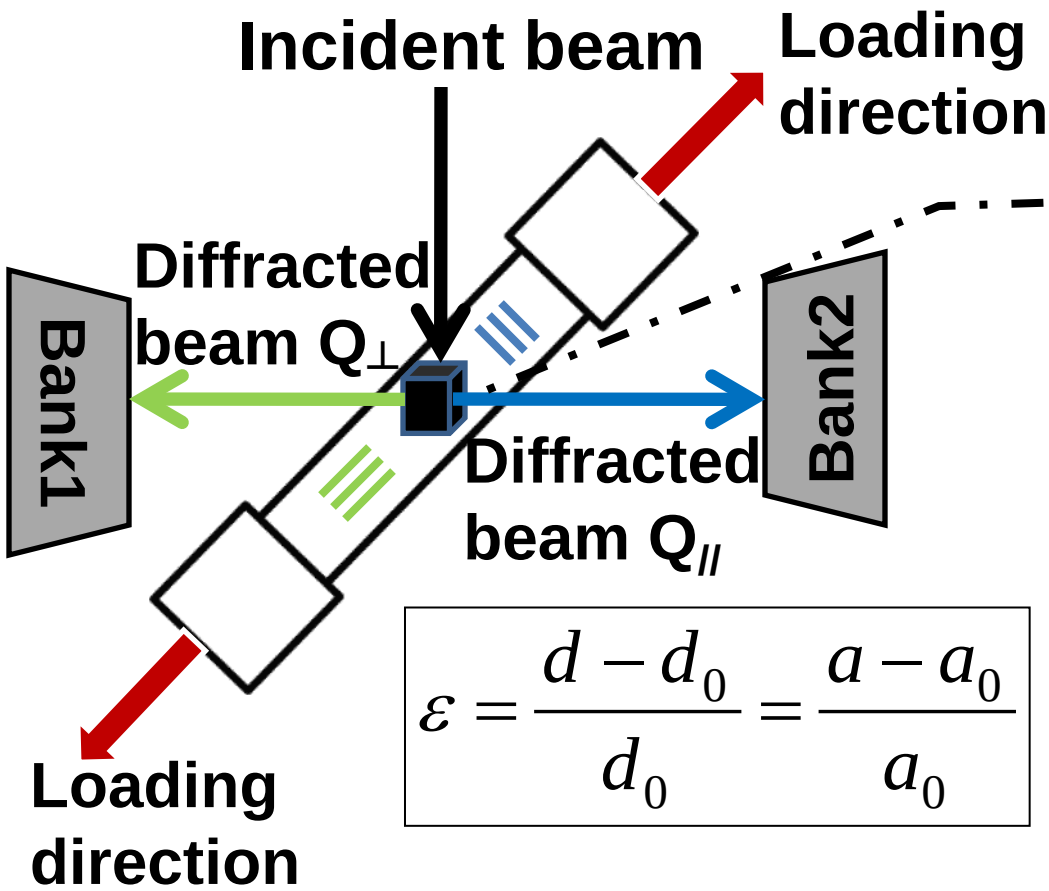

$$\varepsilon = \frac{d - d_0}{d_0} = \frac{a - a_0}{a_0}$$

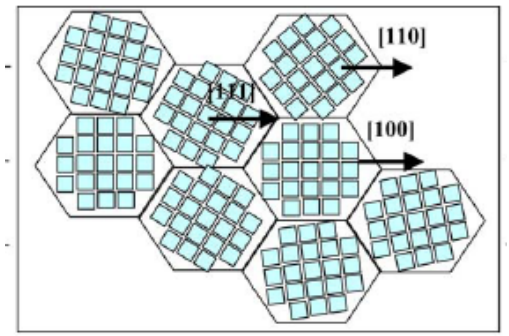

Phase strain

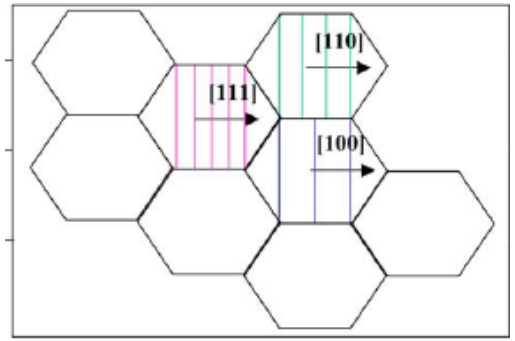

Plane specific strain

Neutron diffraction provides direct measurements of elastic strains (lattice strains). Peak position, width, and intensity are obtained.

3.6 Proposed Research: Neutron-Diffraction Studies

- Information directly and indirectly (coupled with finite element modeling) determined by in-situ neutron diffraction during tension and creep:
  - Lattice strain (phase and hkl plane-specific strain) and stress
  - Lattice misfit between the matrix and precipitates
  - Phase volume fractions
  - Texture evolution during deformation
  - Load partitioning among phases
  - Elastic moduli of constituent phases
  - Critical resolved shear stress

4.1 Proposed Research: Creep Experiments

1. Extend measurements for FBB6 (10^{-4} – 10^{-9} s^{-1})

- Compression Creep
  effect of stress 40-200 MPa (stress exponent)
  effect of temperature 600-700 ºC (activation energy)
- Tension Creep
  effect of stress 40-200 MPa (stress exponent)
  effect of temperature 600-700 ºC (activation energy)
  measure primary creep
  measure tensile ductility + fracture time
- Model Creep
  Simple creep equations
  Dislocation dynamics
  predict optimal microstructure
- Microstructure before and after creep
  Grain size
  Precipitate size and spacing
  Ambient tensile properties

$$\dot{\varepsilon} = A\sigma^n \exp\left(-\frac{Q}{RT}\right)$$

$$t_f \dot{\varepsilon} = C$$

$$\frac{t_f \dot{\varepsilon}}{\varepsilon_f} = C'$$

2. Perform above measurements on new alloys

Dislocation Models – Closed Form Solutions

1. Precipitate Shearing
   a. Elastic interactions:
      i. Lattice parameter misfit (δ)
      ii. Shear modulus mismatch (Δμ)
   b. Order (γ_{APB})

2. Orowan looping (bypass)

1ai. and 1aii. : ***additive***

1a. and 1b. : ***series*** (larger prevails)

1. and 2. : ***parallel*** (smaller prevails)

$$\Delta\tau_{coh} = \alpha_{\varepsilon}\left(\mu|\varepsilon|\right)^{3/2}\sqrt{\frac{\langle r\rangle\phi}{\mu b/2}}$$

$$\Delta\tau_{\mathrm{mod}} = 0.0055\,\Delta\mu^{3/2}\sqrt{\frac{2\phi}{\mu}}\left(\frac{\langle r\rangle}{b}\right)^{(3m-2)/2}$$

$$\Delta\tau_{ord} = 0.81\frac{\gamma_{APB}}{2b}\sqrt{\frac{3\pi\phi}{8}}$$

$$\Delta\tau_{Or} = \frac{0.4\,\mu b}{\pi\sqrt{1-\upsilon}}\left[\frac{\ln\left(2\bar{r}/b\right)}{\langle r\rangle\left(\frac{1.538}{\sqrt{\phi}}-1.643\right)}\right]$$

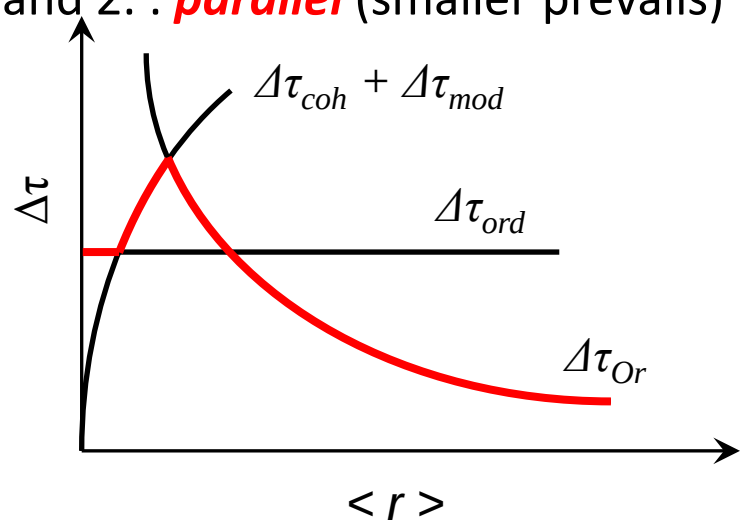

27

Our Precipitate Structure

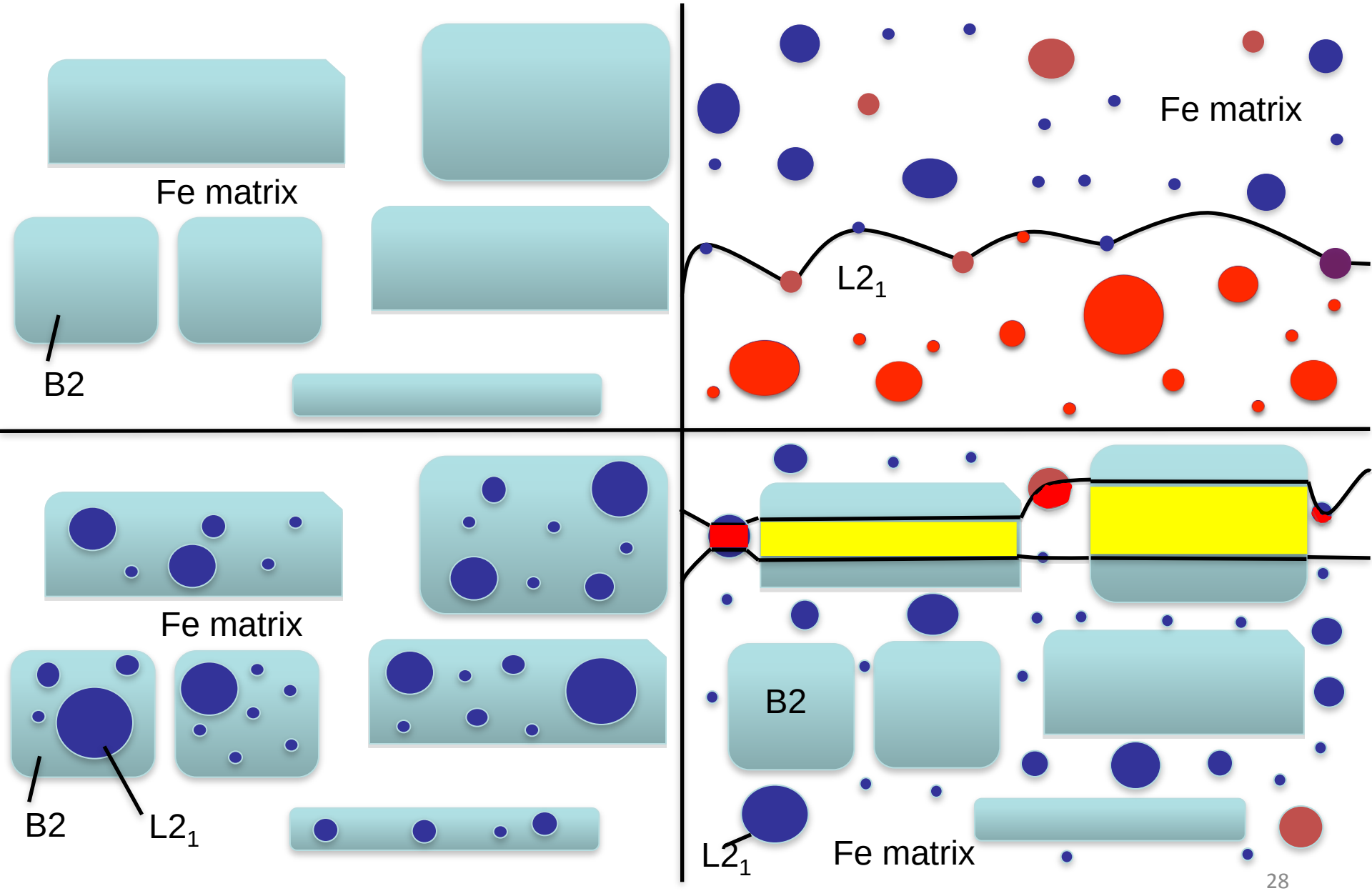

Dislocation-Dynamics Modeling: Method

Mohles V. Phil. Mag. A 2001;81:971

$$\tau_{ext} = -\left(\tau_{disloc} + \tau_{drag} + \tau_{obst}\right)$$

imposed, incremented throughout simulation

disloc. self-interaction stress

internal friction of the lattice

interaction stress between disloc. and precipitate

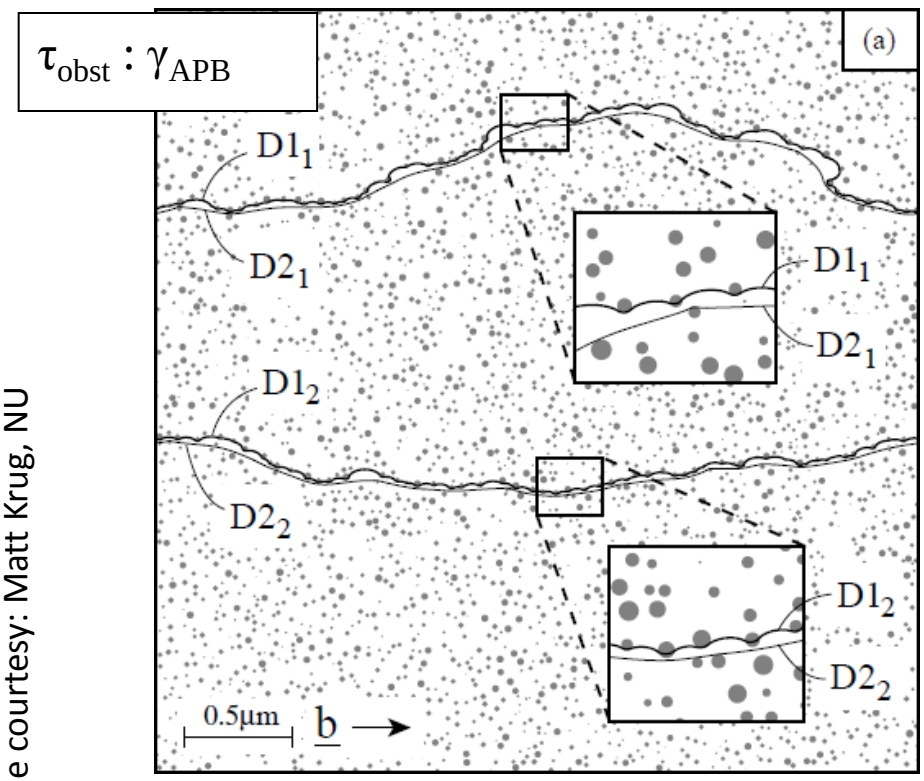

V. Mohles Mater. Sci. Eng. A, 365, 144 (2004).

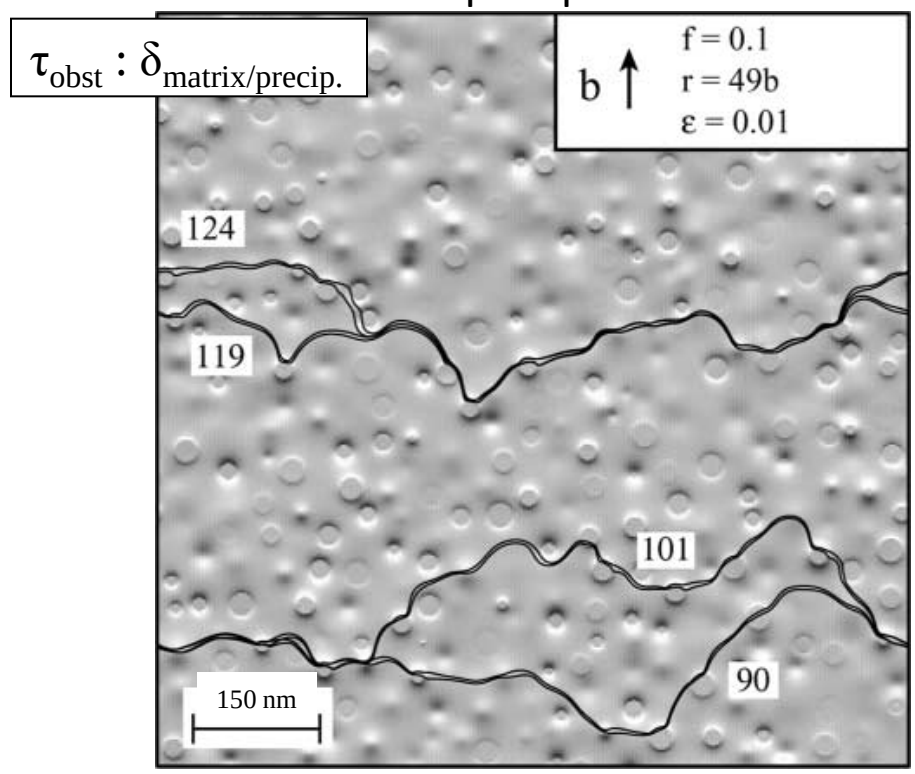

V. Mohles, and E. Nembach. Acta Mater., 49, 2405 (2001).

Slide courtesy: Matt Krug, NU

Dislocation-Dynamics Modeling: Capturing the Dataset

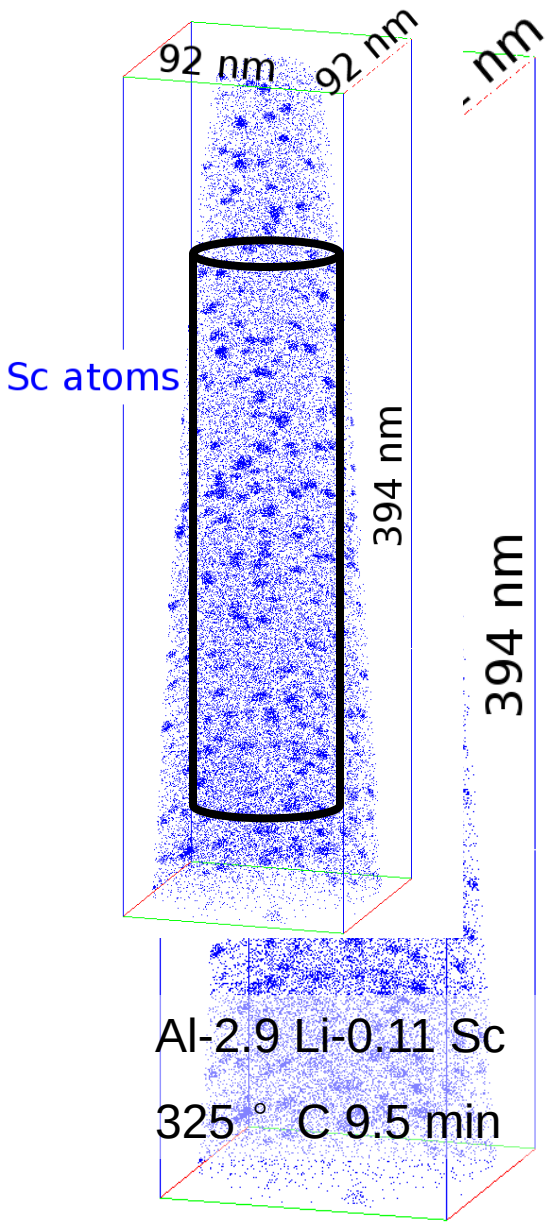

1. Isolate precipitates- cluster search algorithm:

   Each precipitate i : $(x_i \;\; y_i \;\; z_i \;\; r_i)$

- Find largest inscribed cylinder
- Apply random symmetry operations:

  rotations, mirrors, translations
- Assemble resulting cylinders
- Cut through common plane to create glide plane

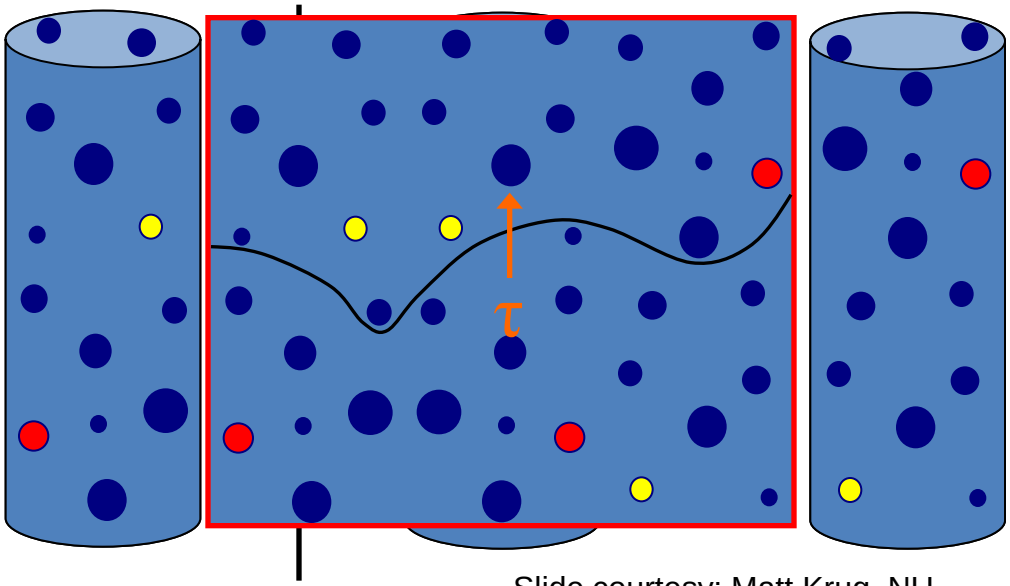

Slide courtesy: Matt Krug, NU

Dislocation-Dynamics Modeling: Example APT Dataset

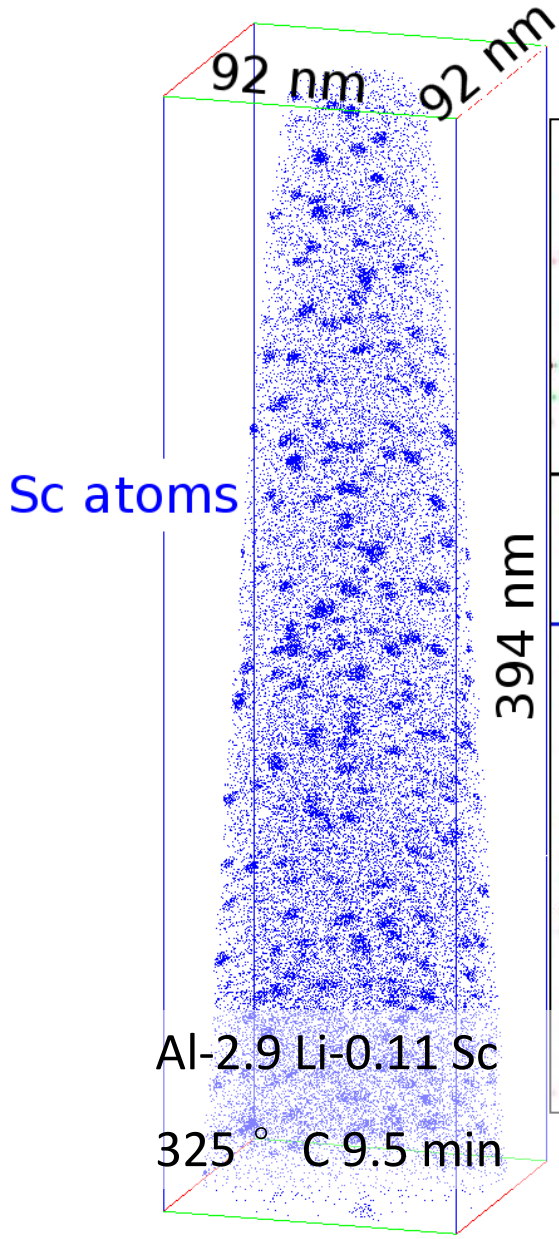

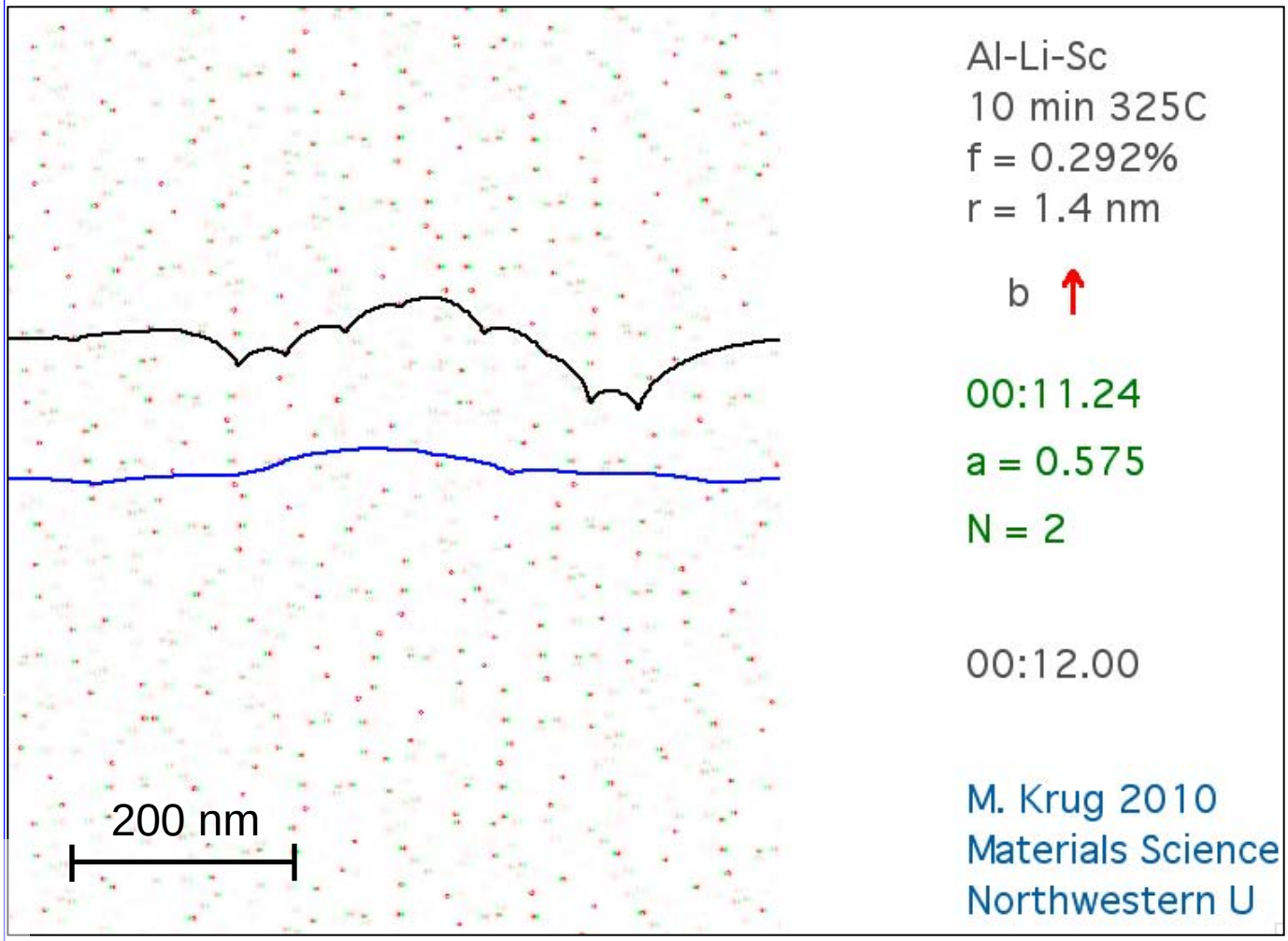

Dislocation-Dynamics Modeling: Example APT Dataset

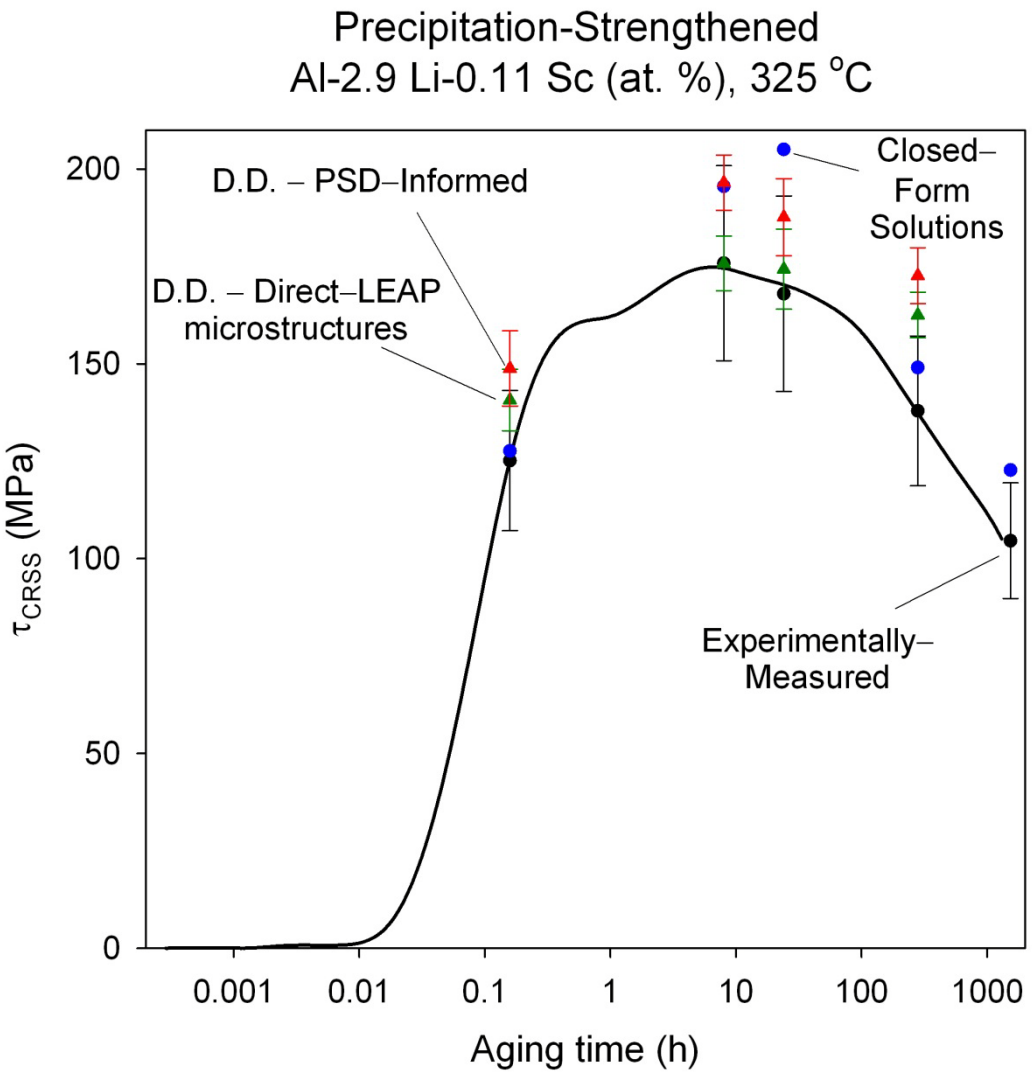

- Closed-Form solutions do well for under- and over-aged, overshoot and miss peak strength
- Particle size distribution (PSD)-informed: overshoots consistently
- Direct LEAP microstructures: captures underaged and peak, overshoots overaged strength.

Slide courtesy: Matt Krug, NU

Strength Modeling

- LEAP-measured datasets simulated
- Model extended to allow:
  1. Modulus strengthening
  2. Multiple strengthening mechanisms simultaneously
  3. Core/shell precipitate structures
- Preliminary results are encouraging for the Al-Li-Sc
- Expand the model to complex steel microstructures

Conclusions

- The proposed B2 or/and $L2_1$ precipitates strengthened ferritic alloys are promising for the elevated-temperature applications.
- Modern computational tools and algorithms will be developed and integrated to promote the development of novel high-temperature alloys for fossil-energy applications.
- Creep experiments, advanced characterizations , and quantitative modeling will be conducted to achieve a fundamental understanding of the creep behaviors of novel ferritic alloys and validate computational results.

Project Tasks

- Task 1: Integrated Design
- Task 2: Thermodynamic Modeling of Multicomponent, Multiphase Alloys
- Task 3: Kinetic Modeling of Multicomponent Alloys
- Task 4: Preparation and Processing of Prototype Alloys
- Task 5: Microstructural Characterization
- Task 6: Creep Behavior

2.7 Proposed Research: Parameters for Dislocation Dynamics Models

- Parameters for solid-solution strengthening
  - Misfit parameters and composition-dependent elastic constants for elastically mediated solute-dislocation interactions

- Parameters for dislocation-precipitate interactions
  - Composition dependent stacking-fault and antiphase-boundary energies for ordered intermetallic phases, important for processes involving shearing of dislocations
  - Composition-dependent lattice parameters and elastic moduli for elastically-mediated interactions

Ferritic Superalloys as a Materials System

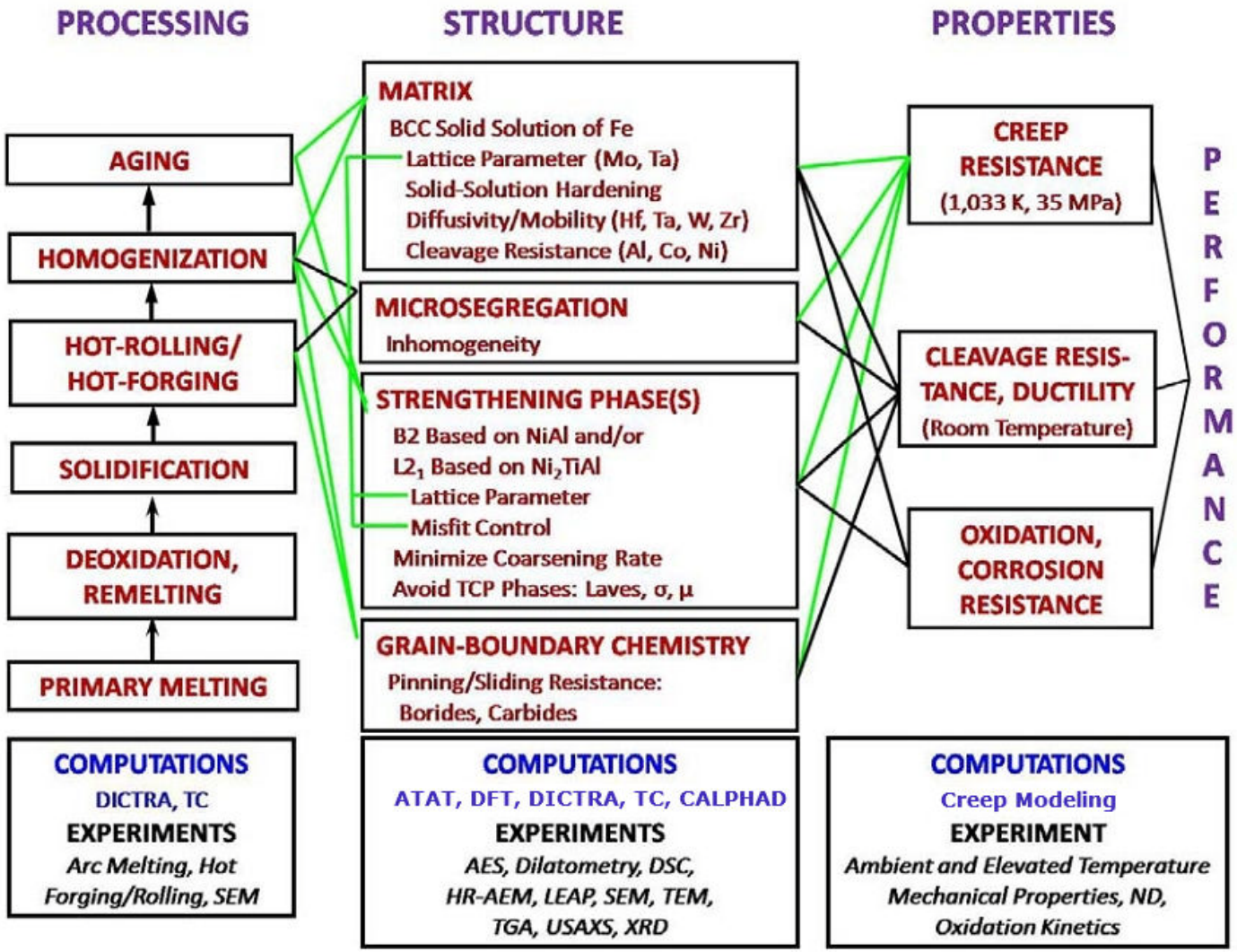

TC: Thermo-Calc; DICTRA: DIffusion Controlled TRAnsformations; DFT: Density Functional Theory; ATAT: Alloy Theoretic Automated Toolkit; CALPHAD: Calculation of Phase Diagrams; HR-AEM: High-Resolution Analytical Electron Microscope; LEAP: Local Electrode Atom Probe; SEM/TEM: Scanning/Transmission Electron Microscope; TGA: Themo-Gravimetric Analysis; USAXS: Ultra-Small-Angle X-ray Scattering;

XRD: X-ray Diffraction

Role of Participants

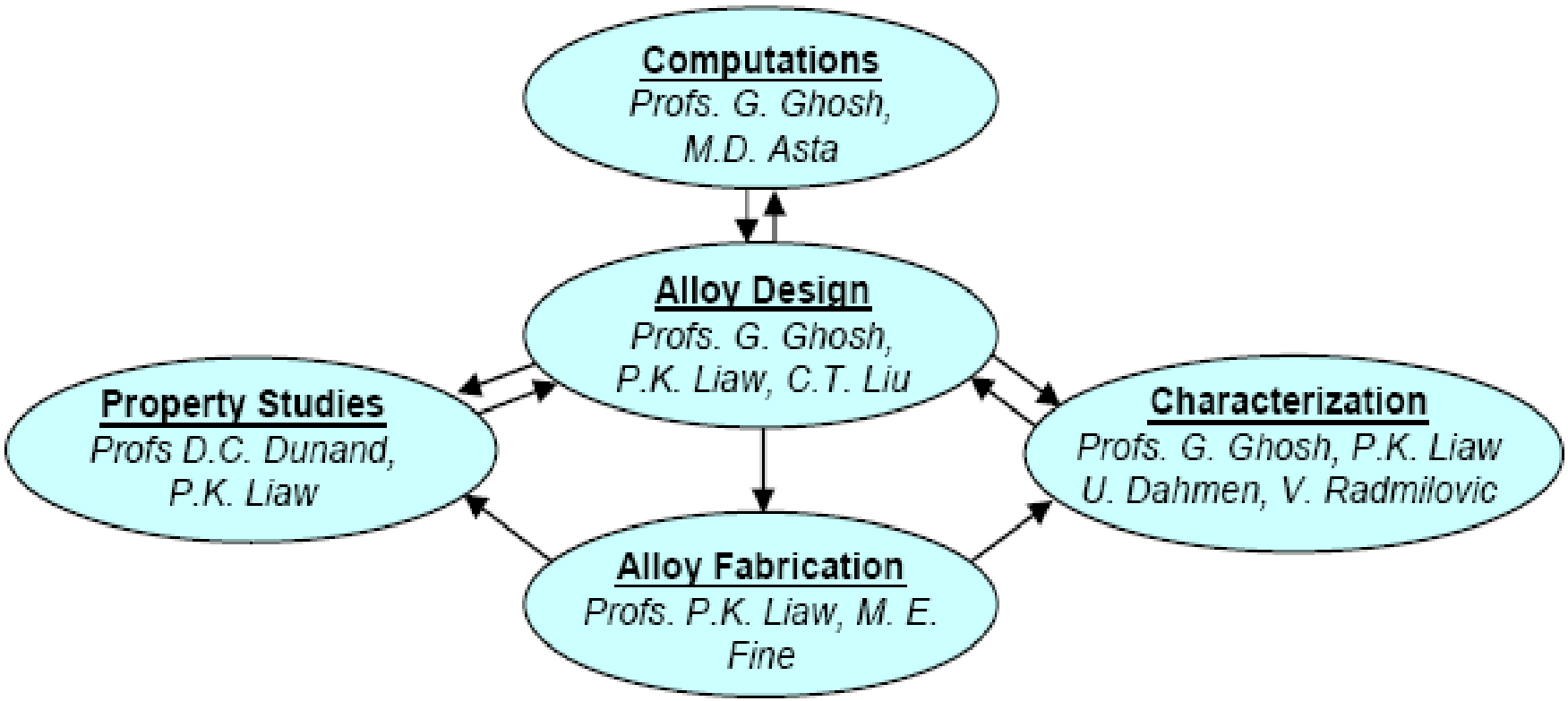

Schematic flow chart illustrating the roles of the participants and the integration of the activities in the computation-based alloy-design project

Ferritic Alloys as Candidates for Steam Turbine (2)

Why not conventional carbide-strengthened ferritic steels?

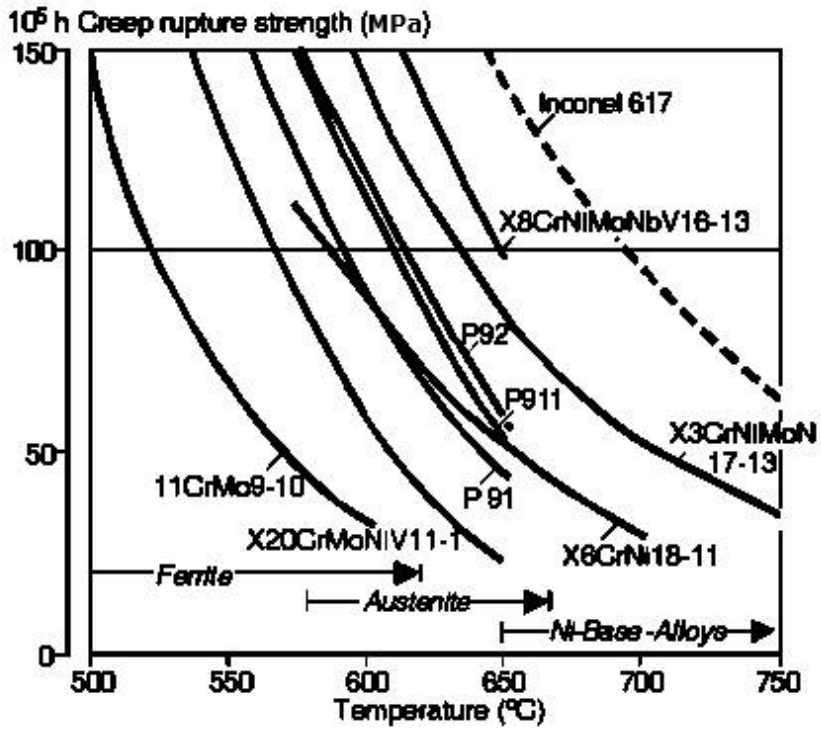

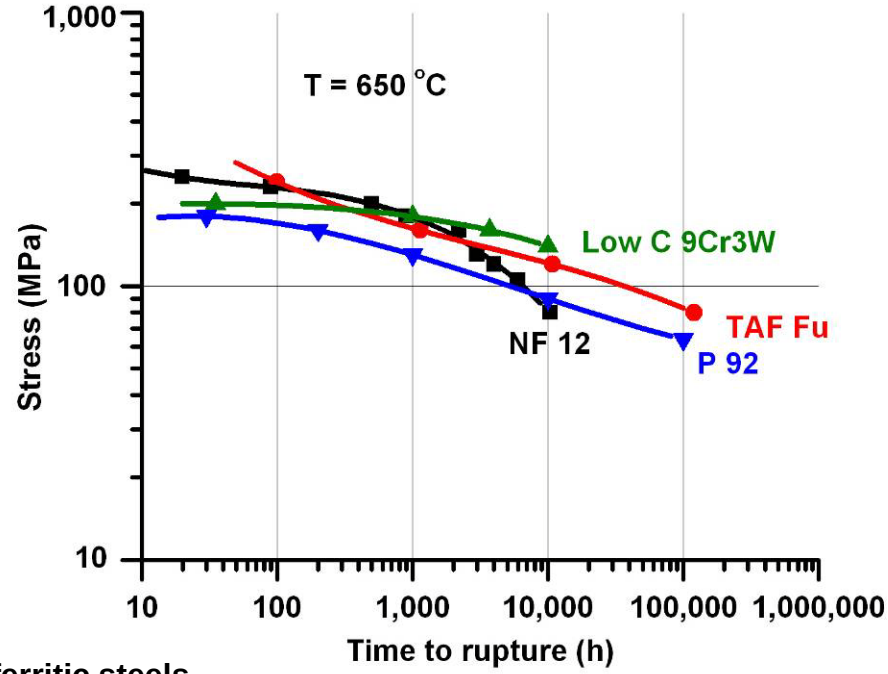

Compositions of the recently developed creep-resistant ferritic steels

Alloy	C	Si	Mn	Al	Cr	Ni	Mo	W	V	Nb	B	N
T/P91	0.08	0.2	0.3	0.04	8	0.4	0.85	-	0.18	0.06	-	0.03
T/P911	0.09	0.1	0.3	0.04	8.5	0.1	0.9	0.9	0.18	0.06	0.005	0.05
T/P92	0.07	0.5	0.3	0.04	8.5	0.4	0.3	1.5	0.15	0.04	0.001	0.03
NF12	0.09	0.03	0.5	-	12	0.5	0.13	2.6	0.2	-	0.002	0.05
TAF	0.18	0.3	0.5	-	10.5	-	1.5	-	0.2	0.15	0.03	-

P92 (9Cr0.6Mo2W) has moved the application of ferritic steels into the range of austenitic steels. However, in long-term creep tests, those materials exhibited sigmoidal-creep behavior due to the strengthening carbides coarsening or dissolving. So far no ferritic alloys demonstrated superior long-term creep resistance than P92.

2.2 Proposed Research: Correlation Factors

LeClaire's 9-frequency Formalism[1]

$$t_1 = -\frac{\Gamma_2}{\Gamma_2 + 3\Gamma_3 + 3\Gamma_3 + \Gamma_3 - \frac{\Gamma_3\Gamma_4}{\Gamma_4 + 0.512\times\Gamma_5} - \frac{2\Gamma_3\Gamma_4}{\Gamma_4 + 3\times 0.512\times\Gamma_0} - \frac{\Gamma_3\Gamma_4}{\Gamma_4 + 7\times 0.512\times\Gamma_0}}$$

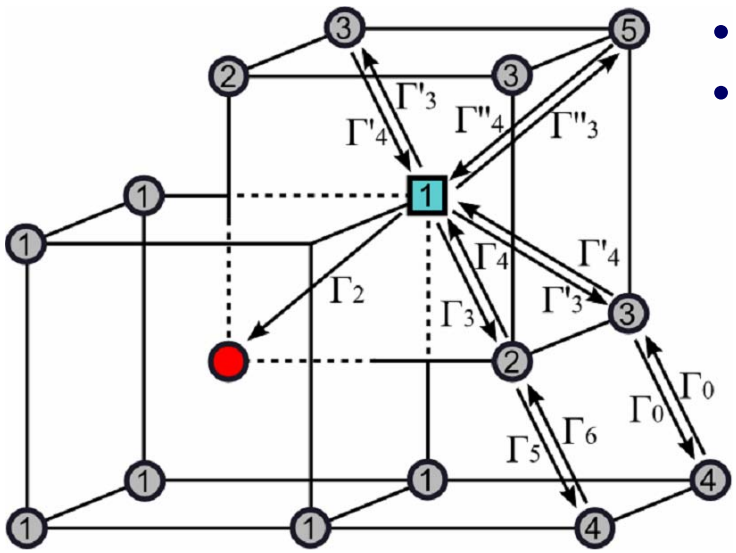

- Migration energies from 1st-principles calculations
- Attempt frequencies assumed constant

Solute	f_{solute} / f_{Fe} @ 1000 K
W	1.02
Mo	0.39
Zr	0.65
Hf	1.12

[1] A. D. Le Claire, In: H. Eyring, editor. Physical Chemistry: An Advanced Treatise, vol. 10. Academic Press (New York), 1970, chap. 5

Preliminary Results

5d Impurity Hf: Preliminary Results

Hf

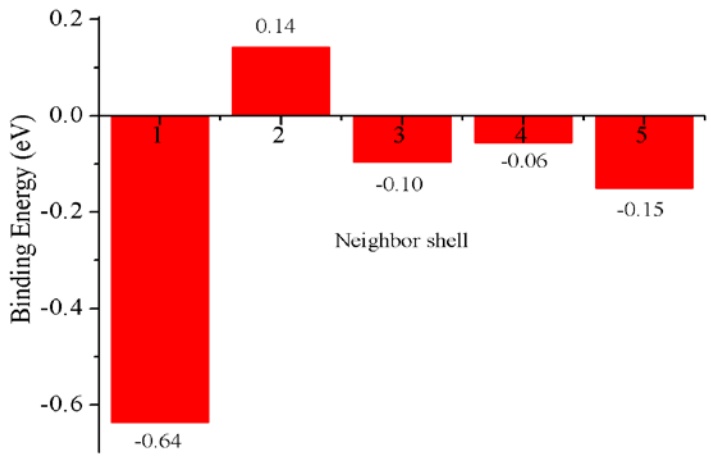

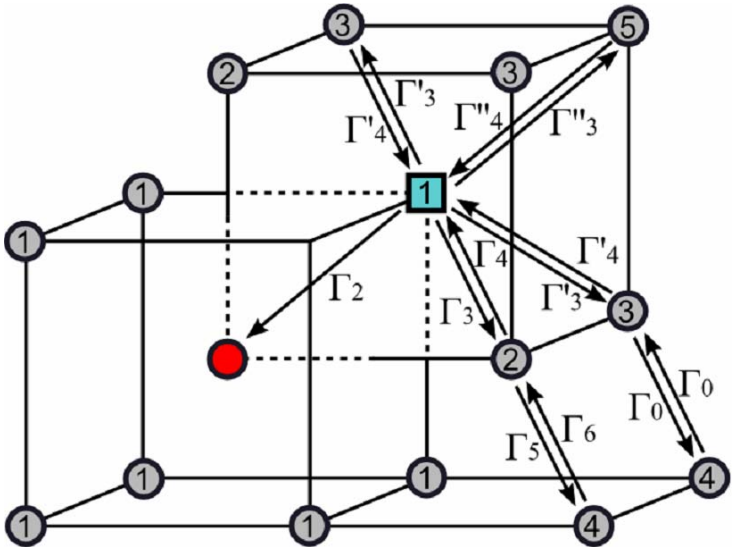

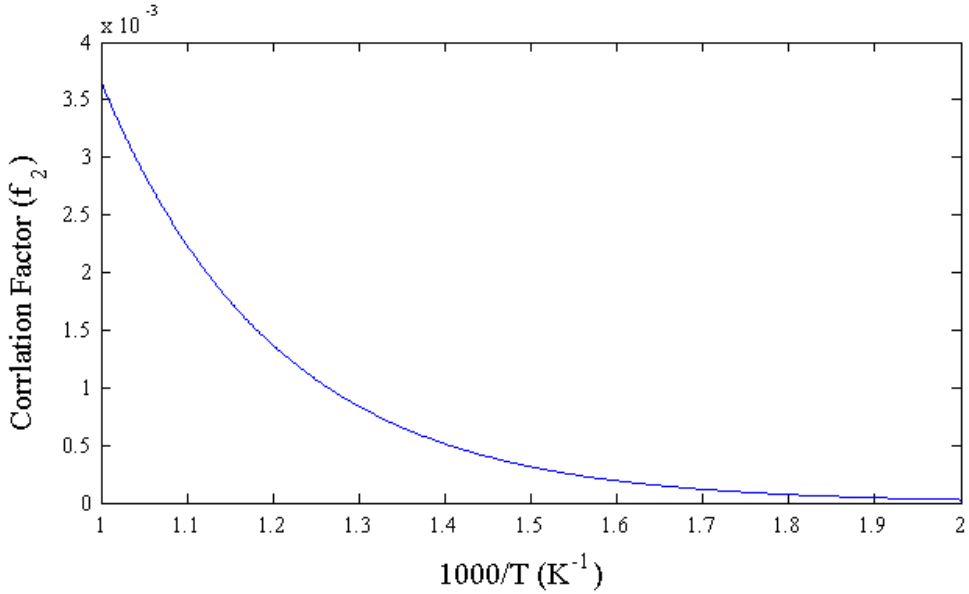

Strong nearest-neighbor binding of solute and vacancy leads to an anomalously small and strongly temperature-dependent correlation factor for impurity diffusion

Anomalous Behavior for Y Impurities

W Impurity: "Normal Behavior"

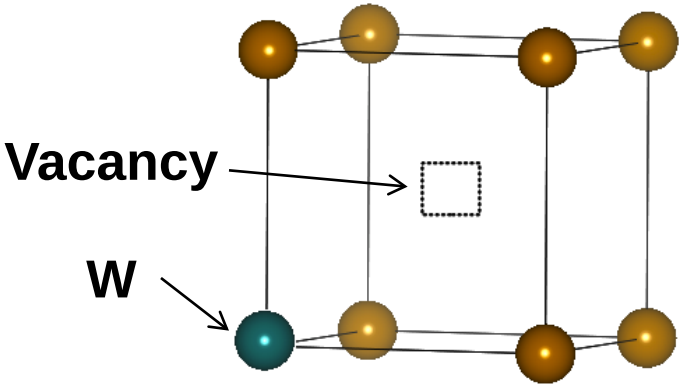

W stable near substitutional site in presence of a vacancy, with saddle point for hop mid-way between substitutional sites

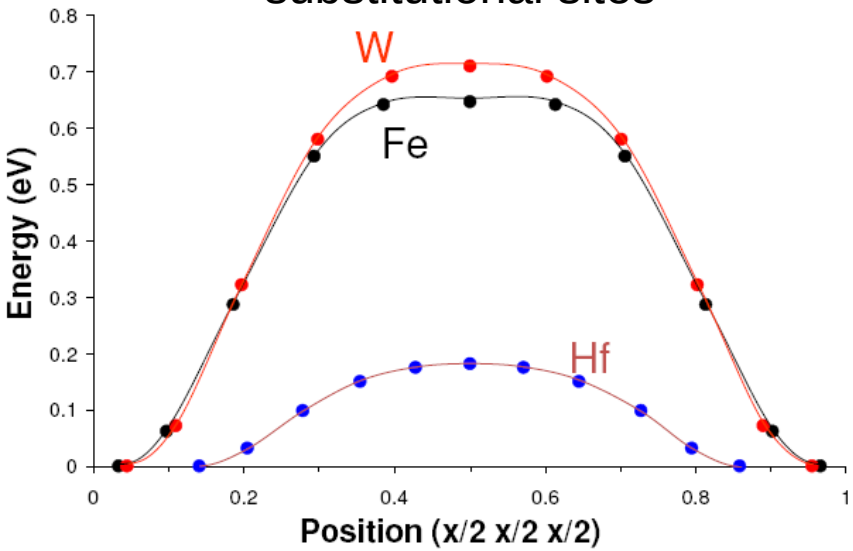

Y Impurity: "Anomalous Behavior"

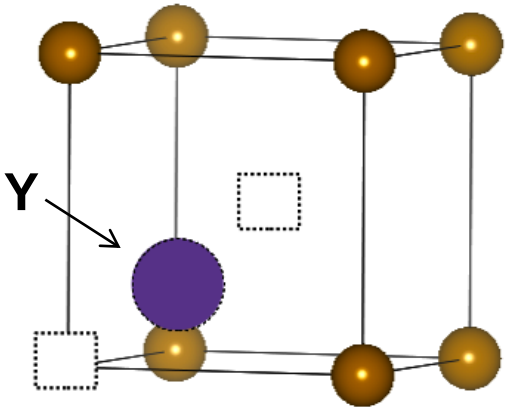

Y strongly bound in position mid-way between substitutional sites, implying fundamentally different and likely higher-energy diffusion mechanism

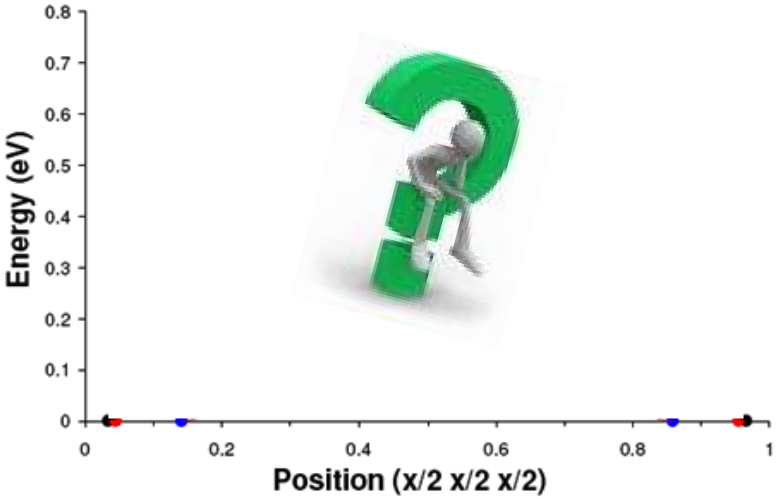

3.3 Proposed Research: Theoretical Model for USAXS Data Analysis

Absolute intensity -- ***Fourier transformation of electron density***

Non-dilute precipitation: Polydispersity + Interference

Difference in scattering-length density between two phases

Scattering from grain boundaries

Number density of precipitates

Incoherent scattering intensity (background)

One population of precipitates

$$I(Q) = n_p |\Delta\rho|^2 P(Q) S(Q) + AQ^{-b} + I_{INC}$$

Form factor – particle size and shape

$$P(Q) = \left(\frac{4\pi}{3}\right)^2 \int F^2(Q,x) \times N(x,R,\delta) \times x^6 dx$$

$$F(Q,x) = [\sin(Qx) - Qx\cos(Qx)]/(Qx)^3$$

$$N(x,R,\delta) = \exp\left[-(x-R)^2/2\delta^2\right]/\sqrt{2\pi\delta^2}$$

Structure factor – inter-particle correlation

$$S(Q,L,\sigma) = 2\left\{\frac{1-\exp\left(-\frac{Q^2\sigma^2}{4}\right)\cos(QL)}{1-2\exp\left(-\frac{Q^2\sigma^2}{4}\right)\cos(QL)+\exp\left(-\frac{Q^2\sigma^2}{2}\right)}\right\}-1$$

Non-linear least-square fitting for 8 parameters: $n_p|\Delta\rho|^2$, I_{INC}, A, R, δ, L, σ, b

2.3 Proposed Research: First-Principles Calculations

- Vacancy Formation, Migration, and Binding Energies
  - VASP, PAW, Spin-Polarized GGA
  - Supercell geometries
- Entropies
  - Harmonic vibrational contributions
  - Electronic contributions included
- Saddle-Point Geometry
  - Mid-point between vacancy and solute neighbors assumed
  - Verified by nudged-elastic-band calculations for W, Fe, and Hf

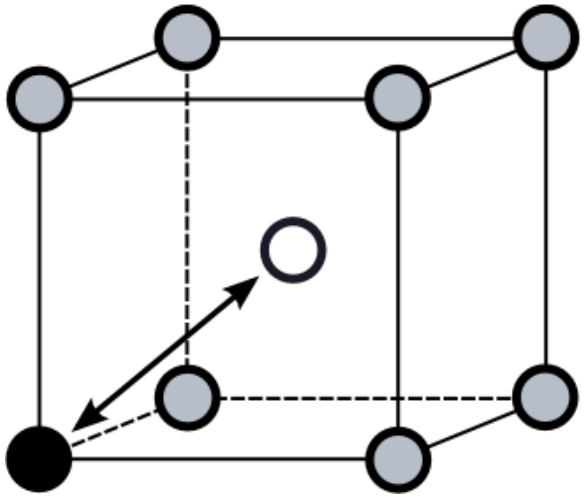

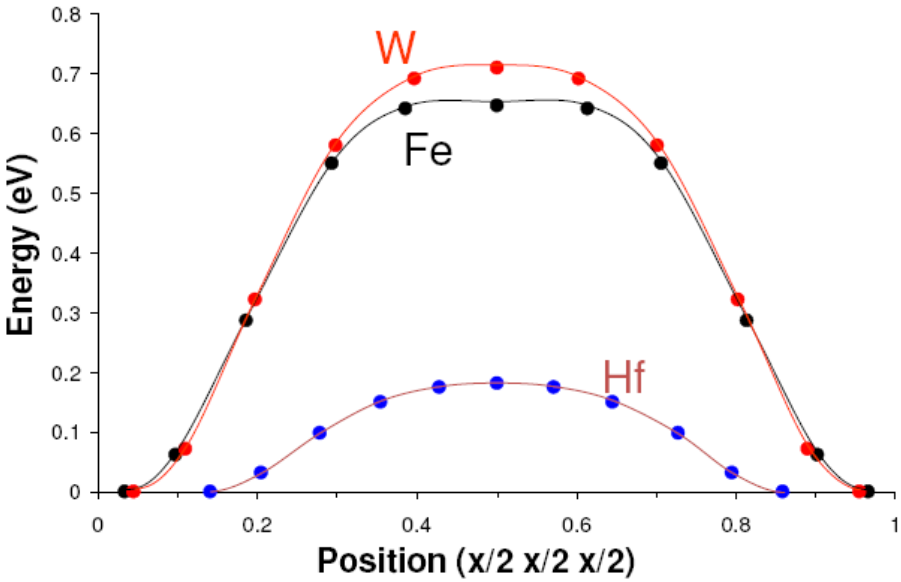

Schematic Diagram of LEAP

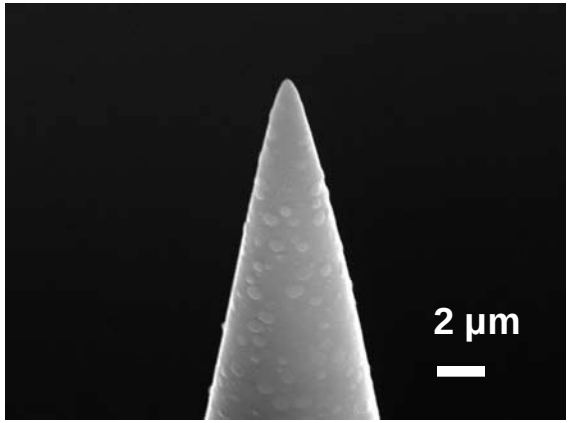

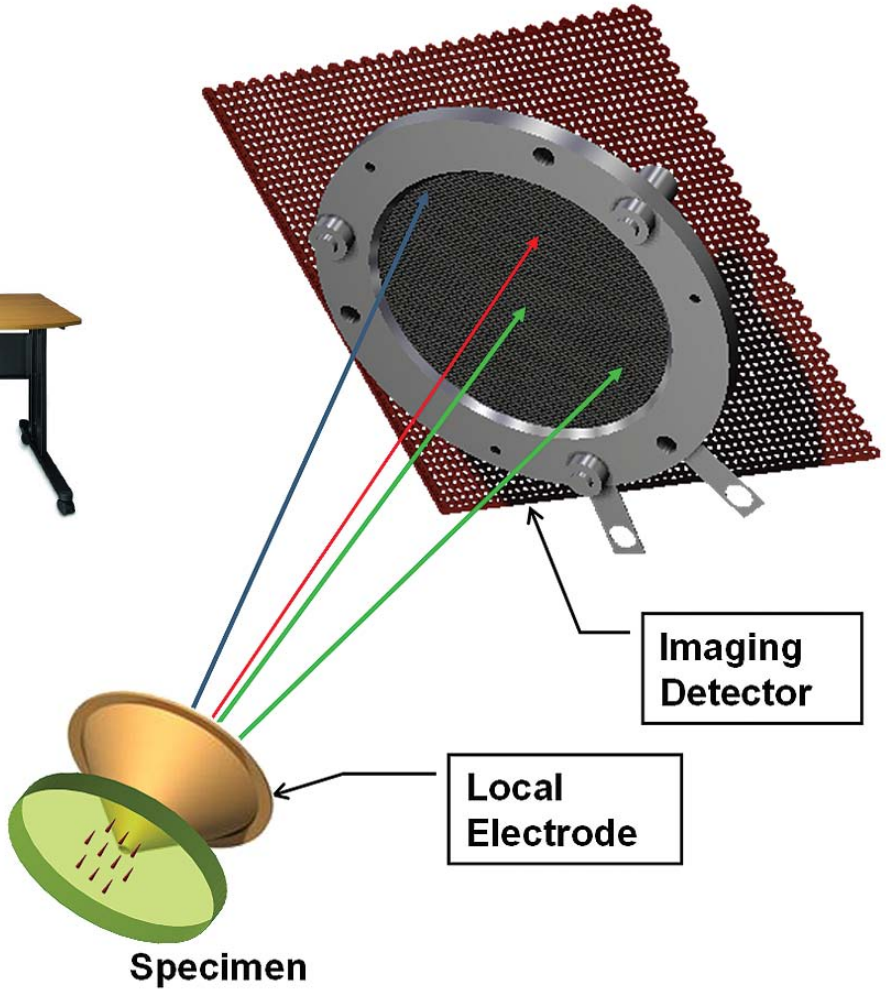

Oak Ridge National Laboratory

D. J. Larson and T. F. Kelly, Imago Scientific Instruments Corporation, Madison, WI, USA

Q & A

Conclusions

Outline

- Technical Background of the Project
- Statement of Project Objectives
- The Project Team
- Previous Results
- Technical Approach to Achieve the Project Goals
- Preliminary results
- Conclusions

1.3 Proposed Research

- Integration of first-principles results
  - Thermo-Calc: multi-component, multi-phase equilibria
  - Thermo-Calc: solid solutions, ordered phase with homogeneity range, ordering energies
    - Predictive accuracy depends on that of database
  - DICTRA: multi-component, multi-phase diffusion
    - Predictive accuracy depends on that of database

1.2 Proposed Research

- Interfacial-energy calculations
  - Sharp interface models: additional calculations using larger supercells are needed to ensure converged results
  - Diffuse interface models: Cluster expansion followed by Monte Carlo simulations will be carried out, and results will be compared with those obtained from sharp interface models

- Composition dependence of elastic constants
  - Analogous to energetics of solid solutions, a cluster-expansion method will be employed to compute the composition dependence of elastic constants (C_{ij}) solid solutions
  - Systems of interest: Fe-Al, Fe-Cr, Fe-Ni, and Al-Ni
  - Elastic constants (C_{ij}) of intermetallics: relevant $B2$ and L_21